

RSG: Fast Learning Adaptive Skills for Quadruped Robots by Skill Graph

Hongyin Zhang[†], Diyuan Shi[†], Zifeng Zhuang, Han Zhao, Zhenyu Wei, Feng Zhao, Sibao Gai, Shangke Lyu*, Donglin Wang*

Machine Intelligence Lab (MiLAB), School of Engineering,
Westlake University, Hangzhou, China.

[†]These authors contributed equally to this work.

*Corresponding authors.

{lyushangke, wangdonglin}@westlake.edu.cn

Abstract. Developing robotic intelligent systems that can adapt quickly to unseen wild situations is one of the critical challenges in pursuing autonomous robotics. Although some impressive progress has been made in walking stability and skill learning in the field of legged robots, their ability to fast adaptation is still inferior to that of animals in nature. Animals are born with massive skills needed to survive, and can quickly acquire new ones, by composing fundamental skills with limited experience. Inspired by this, we propose a novel framework, named Robot Skill Graph (RSG) for organizing massive fundamental skills of robots and dexterously reusing them for fast adaptation. Bearing a structure similar to the Knowledge Graph (KG), RSG is composed of massive dynamic behavioral skills instead of static knowledge in KG and enables discovering implicit relations that exist in between of learning context and acquired skills of robots, serving as a starting point for understanding subtle patterns existing in robots' skill learning. Extensive experimental results demonstrate that RSG can provide rational skill inference upon new tasks and environments, and enable quadruped robots to adapt to new scenarios and learn new skills rapidly.

Keywords: Robot Skill Graph, Massive Skills Organization and Query, Massive Skills Inference and Execution, Rapid Skill Learning

1 INTRODUCTION

Animals are born with various fundamental skills to survive in complex and varied wild environments, and can swiftly learn new ones by composing these skills with little effort or experience. For instance, sea turtles are born on the shore but may swiftly pick up the new ability to swim when they first enter the sea by adjusting the way their flippers swing, while most legged animals are naturally able to gallop over various terrains without tripping. In other words, animals never learn these extraordinary abilities from scratch for specific tasks. As observed, the mechanism with which an animal can acquire extra sensorimotor abilities while adjusting to external environments implies that these massive fundamental skills lay a solid foundation for fast learning new skills.

The ability to accurately respond to complex and diverse scenarios and the ability to quickly adapt to new environments and tasks is a key part of robot intelligence and autonomy. However, many existing quadruped robot strategies concentrate on learning from scratch or by transferring a few disposable skills, which is far from animals' behavior intelligence. Animals in nature have a large number of survival skills and can perform skill-related reasoning and execution smoothly and efficiently, which is far beyond the reach of previous methods. In this paper, we investigate developing quadruped robots that can mimic the adaptive behavior of animals in nature by leveraging a variety of massive fundamental skills (or behaviors) to adapt into being-faced varied environments and tasks. By drawing inspiration from the Knowledge Graph (KG) and our previous original concept Skill Graph (1), we propose a new framework called Robot Skill Graph (RSG) for the organization, query, inference, and execution of massive skills for quadruped robots, as well as the rapid learning of novel skills.

The RSG can efficiently organize massive fundamental skills that quadruped robots have already mastered. Given a targeted new environment or task, RSG queries it as input and infers the most appropriate skills as output. The fundamental reason behind this approach is that existing skills in RSG contain plentiful prior knowledge that is valuable for new scenarios, and thus can provide feasible initialization by correctly extracting and coordinating relevant skills. These skills culled from the RSG will serve as a basis for further rapid learning to quickly complete new tasks. Moreover, the resulting new skills will be added to RSG as part of the knowledge for continued learning and evolution in the future. To sum up, the proposed RSG-based motor skill generation mechanism is evaluated on the quadruped robot, which aims to pursue a flexible motion behavior in front of unpredictable changes and meanwhile acquire a fast and flexible adaptive motion capability to new tasks and environments.

2 BACKGROUND

The main goal for Artificial Intelligence (AI) and robotics systems is to achieve human-level intelligence and behaviors. Despite recent breakthroughs of AI in decision-making (2,3,4,5,6), healthcare (7), legged locomotion (8), and content generation (9,10,11) tasks, many of the basic sensorimotor capacities that humans and animals have or acquire effortlessly, remain deceptively challenging for robotic systems (12). This inferiority is partially due to AI systems' fragility to unforeseen changes and lack of ability to interact with unpredictable events (12,13). Therefore, to succeed in a world of unknowns, an agent must adapt to new situations using acquired knowledge.

To achieve this goal, recent learning-based works have made impressive progress in robot behavior adaptation (14,15,16,17), and quadrupedal adaptive motor skills (18,19,20). However, the effectiveness of their approaches has not been evaluated in situations where massive skills need to be stored and reused. Robots are still far from animal-level controlling in terms of flexibility and stability, especially when encountering new environments. Therefore, it is worth understanding how animals produce adaptive reactions in unseen environments. In fact, animals are not only born with many necessary core skills, but they are also able to dynamically extract basic skills from

limited experience and combine them into more advanced skills, allowing them to quickly adapt to new situations. These impressive skills in animals were never trained from scratch for specific tasks but instead generated from basic skills or past experiences. The ability of animals to rapidly develop the sensorimotor skills needed to adapt to new environments suggests that core fundamental skills provide a solid foundation.

Recently, interest in research in Deep Reinforcement Learning (DRL)-based robot motion control has been drawn into ways to avoid learning from scratch. Lee et al. (21) first utilized DRL to train the robot’s self-recovery, standing, and walking behaviors and then employed a behavior selector to perform downstream tasks. Yang et al. (22) leveraged a multi-expert learning approach to integrate multiple basic skills to obtain highly adaptive robotic movements for complex environments. Bohez et al. (23) learned reusable robotic motor skills from animal behaviors for controllable walking and kicking behaviors. Huang et al. (24) first designed specific robot skills, including jumping, diving, and sidestepping, and then trained the high-level planner to complete multi-skill control, and finally realized the robot’s football goalkeeping task. However, these methods lack skill diversity, are difficult to extend to more complex and diverse environments and tasks, as well as difficult to achieve rapid learning of new skills.

3 RELATED WORK

DRL-based Quadrupedal Locomotion: In the realistic DRL-based quadrupedal locomotion research, prior knowledge is represented in a variety of forms, such as motion data (25,26,27), trajectory generators (28,29,30,31) and control methods (32,33,34). Motion data is often generated by other sub-optimal controllers or directly acquired from public datasets. By utilizing motion data directly as a reward function or adversarial motion priors (35,36,37), the robot could obtain natural and agile motion patterns to complete specified tasks. Trajectory generators and control methods generally introduce priors into the action space of DRL policies to narrow the search space of actions, which greatly reduces the learning difficulty of the robot and improves its sample efficiency. In our work, the DRL-based learning method is utilized in the fundamental skills collection stage.

Skill-based Reinforcement Learning: In skill-based reinforcement learning (RL), skills are generally represented as sub-policies or a series of low-level actions to facilitate learning long-horizon behaviors. Many works propose instructing agents to take action as temporal-extending skills, such as options (38,39,40) or motion primitives (41,42,43,44,45,46,47,48). Intuitively, temporal abstraction can effectively reduce the task horizon of the agent and enable directed exploration, which is a major challenge for DRL agents solving challenging tasks (49). However, skill-based RL struggles with more challenging real-world tasks and requires a large number of environmental interactions (50,51). Shi et al. (52) recently used model-based RL to guide skill planning on dexterous manipulation tasks to improve sample efficiency.

Knowledge Graph Embedding: Knowledge Graph Embedding (KGE) (53,54), also known as knowledge graph representation learning, aims to learn latent embeddings of entities, relations, and facts that are extracted from the real-world knowledge

base. Most algorithms focus on developing various models to better describe interactions between entities and relations (54). As a classical translational KGE model, the TransE (55) is proposed to model relations as translation in real-valued vector space, and the TransH (56) model improved TransE by supporting one-to-many, many-to-one, and many-to-many relations better. As newly proposed KGE models, RotatE (57) and DiriE (58) could support more relation patterns. Following KGE, the Knowledge Graph Completion (KGC) is naturally derived by utilizing score functions. In our work, RSG aims to learn representations of skills and relations jointly from pre-defined labels and context similarity. The TransH is utilized to construct relationships among entities because of its simplicity and ability to describe one-to-many and many-to-one relationships that are ubiquitous in this setting. We also utilize KGC to calculate how well new contexts match those skills existing in RSG.

Few-Shot Learning: Few-Shot Learning can recognize unlabeled data (query set) from novel classes with only a few labeled data (support set) by transferring learned knowledge, which can be directly used for fast adaptation. Overall, there are three kinds of methods, including **1)** fine-tuning-based methods tackle the problem by learning to transfer; **2)** metric-based methods (59,60) solve the problem by learning to compare; **3)** meta-based (61) methods address the problem by learning to learn. While such methods can be utilized for the fast adaptation of a few simple skills, our method focuses on the rapid learning of robot skills.

4 RESULTS

Enhancing accurate responsiveness to diverse unstructured environments and rapid adaptability to new scenarios is an important step toward robotic decision-making intelligence. To promote the further development of robot autonomous intelligence, a novel framework called Robot Skill Graph (RSG) is constructed in this paper. The framework can realize the organization, query, and inference of massive fundamental skills, as well as the rapid learning of new skills, as shown in Fig. 1. Fundamental skills are implemented by the trained DRL-based action network. The initial version of RSG contains approximately 320 fundamental skills and takes up about 640MB of storage space. The time complexity of RSG's skill inference is $O(cN)$, which means that it is proportional to the number of fundamental skills N and the number of contexts considered c . In the following sections, we first perform a visual analysis of the RSG construction and representation. Then RSG's skills query, inference, and reuse are illustrated for complex long-time sequential tasks. Finally, we report how to composite the fundamental skills in RSG to enable fast learning of new environments or tasks.

4.1 RSG Construction and Representation

Theoretically, the RSG learns representation jointly from pre-defined link labels and context similarities, where context refers to the environment or task. Pre-defined link labels could be obtained during the skill collection process. For example, the skill of “*forward walking on grassland*” would be linked to the task of “*forward walking*” and

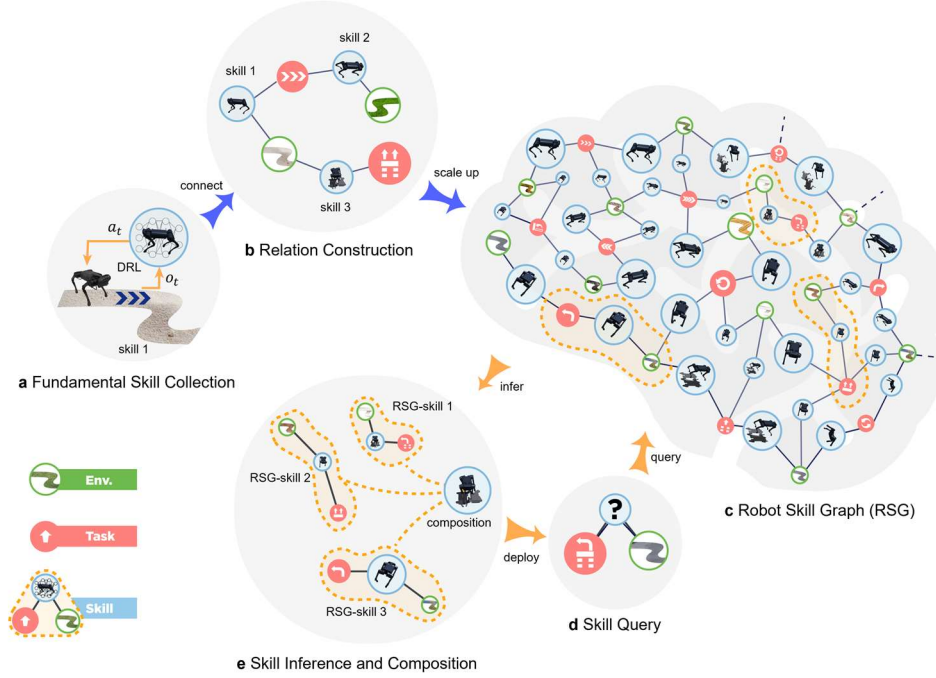


Fig. 1 | Overall framework for the construction and application of RSG. **a**, Collect a rich and diverse set of fundamental skills through the DRL approach with each skill consisting of a task, an environment and a policy network. **b**, Different skills are connected through relationships between environmental entities and task entities. **c**, Illustration of the RSG structure. **d**, Given a new task and environment query, the RSG calculates the match between existing fundamental skills and new required skills. **e**, Finally, these skills inferred by RSG will be executed, composited, or fine-tuned respectively according to the matching degree. The newly learned skills will be also added to RSG for future usage.

the environment of “grassland”. The context similarities are calculated from the inherent physical properties of context entities, such as the friction coefficient of the environment or trajectory of the robot body’s Center of Mass (CoM). The utilization of context similarity enables context to be generalized and new context-skill links automatically discovered. While pre-defined labels are utilized to incentivize the RSG to classify context instances into the corresponding context classes and learn more semantic representation. For example, given three environment instances $Env_a = (0.65, 3.0, 0.0)$, $Env_b = (0.65, 0.0, 0.0)$, and $Env_c = (0.65, 7.0, 0.0)$. Similarity-based methods would yield higher similarity scores for Env_a and Env_b , because of their higher similarities. While RSG,

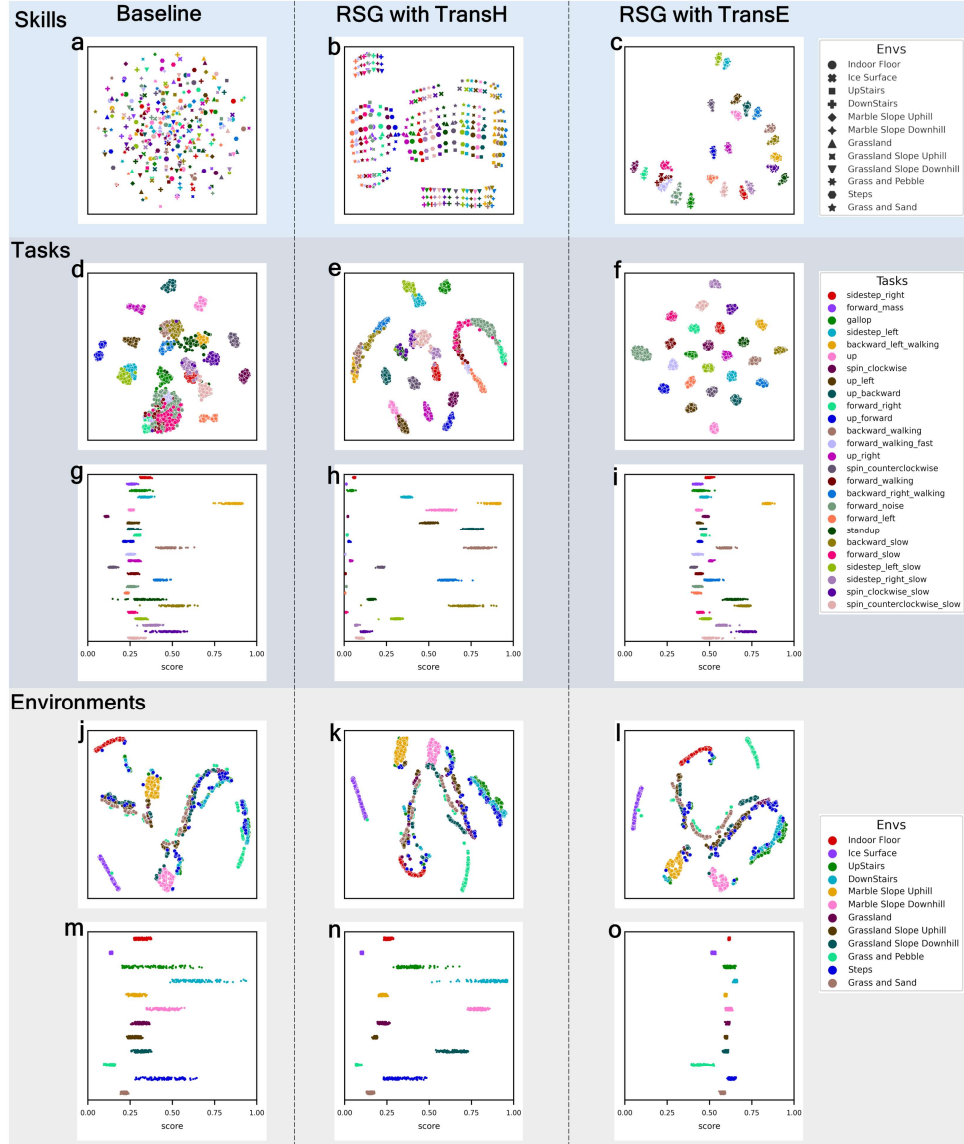


Fig. 2. | Visual analysis of RSG representation and inference. **a-c**, T-SNE visualization of skill embeddings via raw form, RSG with TransH, and RSG with TransE, respectively. **d-f**, T-SNE visualization of task embeddings via raw form, RSG with TransH, and RSG with TransE, respectively. **g-i**, Task cross scores of *backward left walking* on *grassland* via KNN, RSG with TransH, and RSG with TransE, respectively. **j-l**, T-SNE visualization of environment embeddings via raw form, RSG with TransH, and RSG with TransE, respectively. **m-o**, Environment cross scores of *forward walking* on *downstairs* via KNN, RSG with TransH, and RSG with TransE, respectively.

employing class information, could deduce that Env_a and Env_c belong to the class of “Grassland” and hence share skills between them.

Practically, the RSG could be utilized for the following two tasks naturally and effectively: **1) Skill mining:** by performing the RSG representation learning on existing skills and their contexts, we could discover missing links and ease the need for training new skills. It is achieved by KGC in a straightforward way. By calculating existing skill scores for all other possible contexts in the RSG, a new link with a high score indicates a high probability of reusing this skill in that context; **2) Skill inference:** by querying the RSG using (potentially unseen) context, the RSG is able to quickly infer fundamental skills that closely match the new skills. Furthermore, we utilize context encoders and train the RSG with similarity-aware loss to achieve generalization of context properties, which may be difficult to achieve in normal knowledge graph settings.

4.2 Analysis of Skill Graph

We primarily conduct two types of experiments to compare the proposed RSG and baseline methods. One is the t-SNE analysis to visualize the representation space and the other is the context cross scores in which we test how a given method assigns a score to a different context. In our proposed RSG, the TransH method is utilized by default, i.e. RSG with TransH. We compare it against a baseline method, RSG with TransE, where the TransH is replaced by TransE. In cross scores experiments, we also compare to k-nearest nearest neighbors (KNN)-based baseline.

In Fig. 2(a-c, d-f, and j-l), we employ t-SNE analysis to visualize representation learned by several methods and observe that: **1)** Raw representations (in skills, tasks, and environments, as shown in Fig. 2a, d, and j) are both scattered and clustered, which requires the algorithm to consider both similarity and semantic information; **2)** As shown in Fig. 2e, the RSG correctly captures the original relationships of context samples. More importantly, our method can learn semantic representation. The RSG could separate points of “forward noise”, “forward right”, “forward left”, “forward walking fast” and “forward walking”, which are similar to each other and mixed in raw t-SNE, into different clusters with clearer boundaries. Thus, by learning predefined link labels and context properties together, the RSG can discover semantic representations. **3)** Learned representation of RSG with TransE tends to be totally scattered with no mixings observed, especially in Fig. 2f. The reason is that if two context points get too close, the TransE cannot map them into different skills by its inherent inductive bias. Such a phenomenon is also reflected in Fig. 2c, where the RSG with TransE is not aware of the differences among environments, but only distinguishes skill representations by task dimensions. On the contrary, our presented RSG could separate skill representations in both dimensions, as shown in Fig. 2b.

Furthermore, we designed the experiment to investigate how these methods would assign scores of the given skill to new contexts. Fig. 2g-i are obtained by calculating scores of “backward left walking on grassland” to other task contexts, where underlined words mean the scores are computed in task dimension via replacing *backward left walking* with other possible tasks. Fig. 2m-o are in similar settings, except that we compute “*forward walking* on Downstairs” scores for other environmental contexts. These



Fig. 3 | Real-machine deployment of (partial) fundamental skills in RSG. Robot motion tasks include rolling, standing, walking, turning, small steps, etc. The environment includes unstable debris, narrow passages, single-plank bridge, sponge mat, dirt piles, lawns, muds, pebbles, stairs, soft clays, etc.

results show that: **1)** Vanilla KNN methods lack the ability to consider semantic class information and yield scores with more overlapping distributions, as shown in Fig. 2g, m; **2)** The RSG with TransE cannot distinguish various contexts, resulting in poor separation performance (Fig. 2i, o); **3)** Our proposed RSG is the only method that shows both correct assignments of low scores to non-related contexts and high scores to highly related contexts. In addition, score ranges of different classes overlap less, as shown in Fig. 2h, n. More analysis can be found in Section S1 and Figures S1-S4.

4.3 Skill Query, Inference and Reuse

Diversity fundamental skills in RSG

In this section, we first demonstrate the multiplicity and effectiveness of the fundamental skills in RSG, in accordance with various environments and tasks, when deployed in the real world. As shown in Fig. 3 and Video S1, quadrupedal robots equipped

with RSG can perform diverse behaviors such as rolling, standing, walking, and turning in the real world. Scenarios that the robot can successfully traverse include a variety of hand-designed rugged surfaces indoors, as well as challenging unstructured terrain in the wild. These natural environments contain deformable terrains, over-ground obstructions, slippery surfaces, and highly irregular profiles.

Stable traverse of rough and unstructured terrain is one of the fundamental and necessary abilities for the legged robot. Dominated by the RSG, the quadrupedal robot can locomote with grace and efficiency, and successfully get over a wide variety of terrain (Fig. 3a-f). This traversal ability is improved by RSG's ability to dynamically infer matching fundamental skills based on changes in environmental information according to the existing environmental entity relationship, to generate behavioral actions that adapt to the current environment. Compared with previous work (21-24), explicitly inferring from strongly correlated skill relationships provides additional advantages in terms of stability and interpretability, which are crucial for robot action generation that requires high robustness and flexibility.

An important criterion for robots to be highly autonomous and intelligent is their ability to handle various tasks in unstructured environments. This ability requires not only stable walking behavior but also flexible and highly dynamic movements. In Fig. 3g-l, Robots equipped with RSG have demonstrated a variety of behavioral skills, including rapidly rolling and standing after external interference, crawling through narrow passages, and walking across single-plank bridges in small steps. These diverse and highly dynamic behaviors are difficult to combine implicitly and efficiently but can be unified under the proposed RSG framework. The RSG is able to perform reasonable and effective skill inference and reuse from a large number of fundamental skills, and perform robust and flexible actions.

Although the fundamental skills in RSG are implemented through DRL-based control policies trained in simulations, these skills have strong enough generalization capabilities to show robust performance in challenging real-world environments and tasks. This guarantees the skill diversity of the RSG that can handle the majority of the common environments and tasks in realistic quadrupedal motion.

Skill inference and execution with precision

To cope with complex and diverse unstructured scenarios, robots' autonomous intelligent decision-making requires a large number of flexible behaviors and efficient skill inference. The construction of RSG is an important step towards fully autonomous and intelligent robots. In this section, we investigate the ability of RSG to infer and reuse fundamental skills based on environment and task queries. Such capability is examined by designing robotic parkours, unstructured long-time sequential tasks, in both simulation and reality (Fig. 4). Difficulties behind the parkour tasks can be roughly summarized as twofold: **1)** each skill to complete the parkour pose different task requirements on the robot and requires it to be capable of inferring the appropriate skills based on the given information and smoothly switching behavior actions accordingly; **2)** the robot must consecutively and successfully accomplish a series of tasks and any task deviation or inappropriate skill extraction may result in the failure of the long-time parkour tasks.

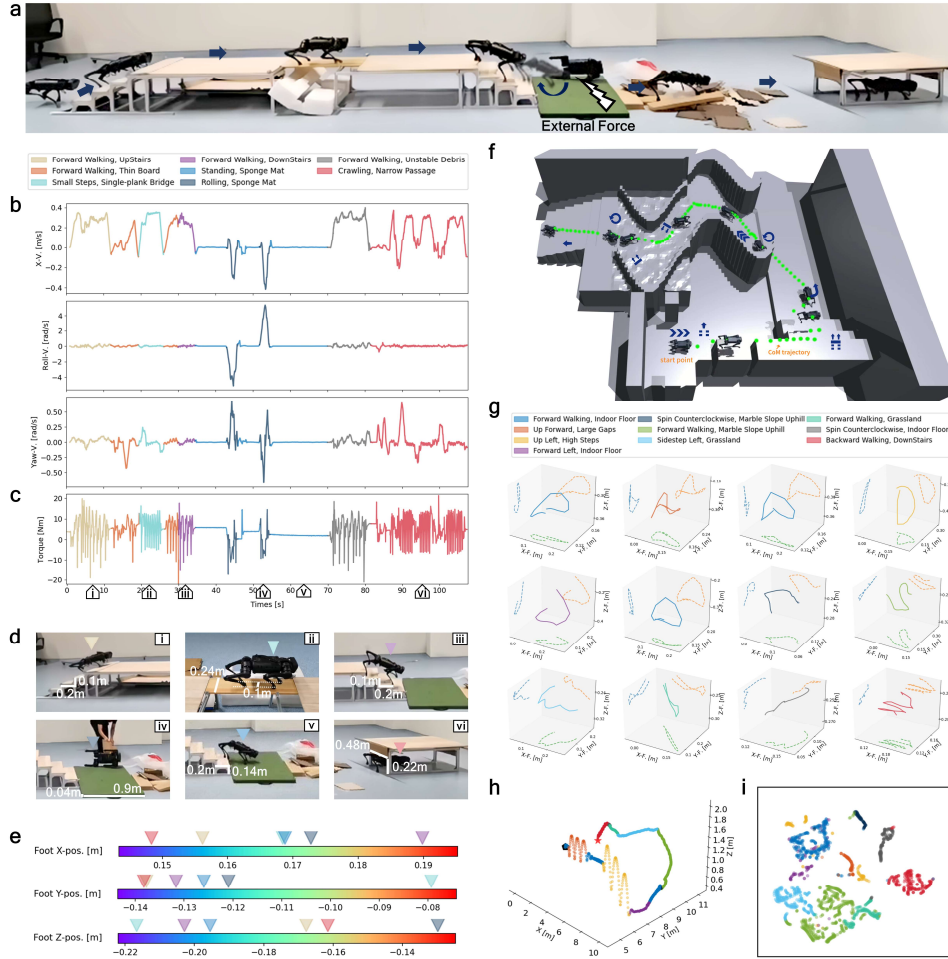


Fig. 4 | The deployment of RSG for robot parkour. **a**, Trajectory on the real robot. **b-c**, The profiles of the robot's body speed and the torque of the front right calf corresponding to **a**. **d-e**, Fundamental skills at six key time nodes, and the average value of the corresponding foot position (right front leg) trajectory. **f**, Ten snapshots during the motion of the robot in simulation. The green dot represents the CoM of the quadrupedal robot. **g**, The foot position trajectory segment of the robot's left front leg corresponding to **f**, and the projections on the three planes XY, XZ, and YZ respectively. **h**, The trajectory of the CoM position of the robot moving. The black pentagon and the red five-pointed star indicate the starting point and end-point of the robot's movement, respectively. **i**, T-SNE visualization of corresponding reused skills.

The parkour map in Fig. 4a consists mainly of stairs (width: 0.2m, height: 0.1~0.14m), single-plank bridges (width: 0.48m), sponge mats (width: 0.9m, height: 0.04m), unstable debris, and narrow passages (width: 0.48m, height: 0.22m). The scenarios are diverse and highly unstructured, requiring the robot to possess a wide range

of skill behaviors. In the parkour task, the robot first walked up the stairs at a speed of about 0.3m/s, with a peak torque of nearly 20Nm (Fig. 4b and c). Then it adjusted its posture and walked across the single-plank bridge in small steps at a speed of nearly 0.4m/s. Compared with other skills, the characteristic of small steps is that its foot position has the smallest Y-axis offset (less than 0.08m, much lower than other skills) and the lowest Z-axis offset (nearly 0.22m), as shown in Fig. 4d(ii) and e. Next, the robot adjusts its gait and walks down the stairs at a speed of about 0.3m/s. The foot position corresponding to its behavior has the largest X-axis offset, which is rather close to 0.19m (Fig. 4d(iii) and e). Then the robot quickly rolled and stood up after being disturbed by two external forces on the sponge mat. Fig. 4b clearly shows the speed changes of the robot during two rolls. Its roll and yaw angular velocity peak values exceed 4rad/s and 0.5rad/s respectively. This skill is characterized by the highest foot position offset, exceeding 0.14m (Fig. 4d(iv) and e). Although the rolling and standing skills are only trained on rigid ground. This suggests that fundamental skills in RSG can cope with more complex scenarios than when training. Subsequently, the robot passed through unstable debris stably at a speed of 0.3m/s, and its torque peak exceeded 20Nm (Fig. 4b and c). In the end, the robot adjusted its body attitude several times before successfully crawling through the narrow passage. its body speed fluctuated between -0.2m/s and 0.4m/s, and the peak yaw angular velocity exceeded 0.5rad/s (Fig. 4b and c). Fig. 4d(vi) and e show that the foot position of the crawling skill has the smallest X-axis offset (less than 0.15m) and the largest Y-axis offset (nearly 0.14m). More realistic results can be found in Figure S5 and Video S2.

For simulated robot parkour (Fig. 4f), several more challenging terrain and tasks were designed, including jumping over the large gaps (interval: 0.1m, width: 0.8m), jumping left sideways down the high steps (width: 0.6~0.64m, height: 0.2~0.4m), spinning on marble slope uphill, and back walking down the stairs. The robot needs to proficiently master various fundamental skills to continuously complete ten different tasks requiring varied gait patterns and properly decide which skills to take. As illustrated in Fig. 4g, foot position trajectory segments, and their projections clearly demonstrate the differences between the skills performed, reflecting the diversity of gait patterns in RSG. To be more specific, the gait pattern of walking on the *indoor floor* is similar to a regular elliptical shape in the three-dimensional space and the corresponding plane projection (*row 2, column 2*), reflecting a certain periodicity of the gait. As the environment and tasks become more complex (i.e., (*row 2, column 4*) and (*row 3, column 3*)), the gait pattern becomes tortuous and irregular to better fit the terrain and match task requirements, which also demonstrates the flexibility and high dynamics of the fundamental skill. In addition, the existence of the jumping motion poses extra challenges in body orientation control and foot placement arrangements. The robot must be able to flexibly and stably manipulate its body when going through various terrains with huge CoM changes, as shown in Fig. 4h. When faced with a large gap, the robot successfully achieves consecutive forward jumps, while performing precise foothold placement, thereby safely jumping over the large gaps and landing stably. During the parkour, all the required fundamental skills need to be clearly distinguished, understood, inferred, and deployed in RSG by robots. In Fig. 4i, the points derived from the same skills are clustered together, and the points of different skills are scattered, which

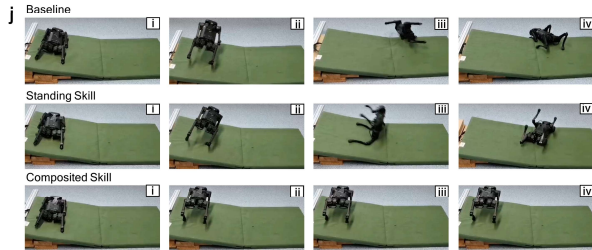
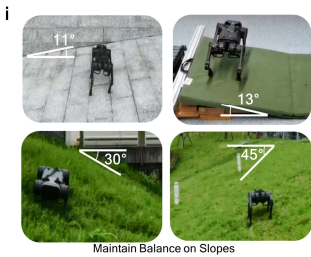
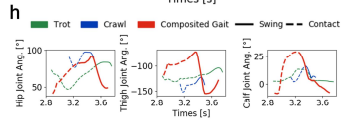
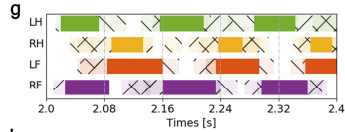
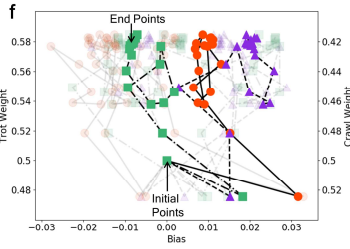
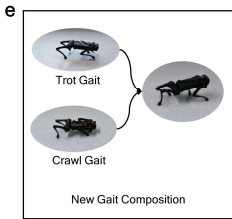
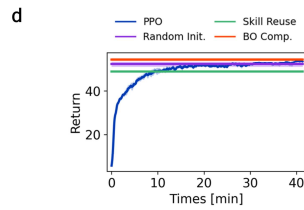
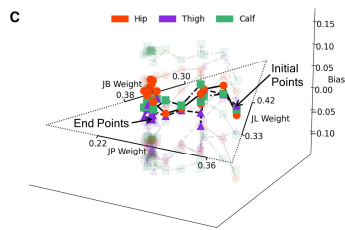
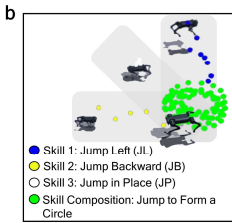
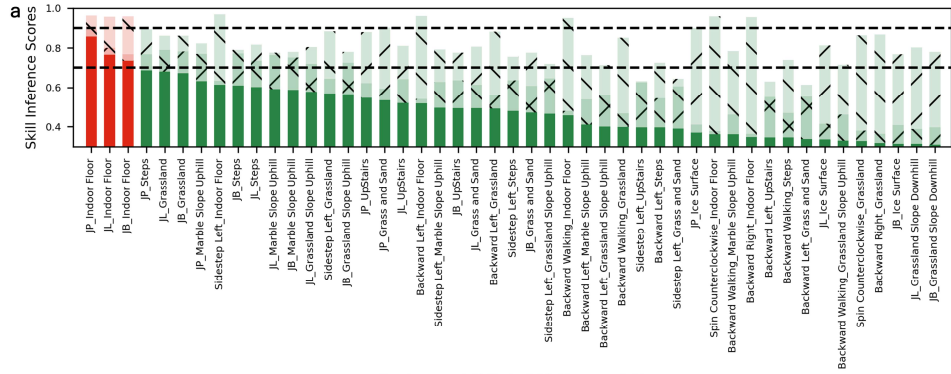
indicates that the different fundamental skills in RSG have been clearly classified. More realistic results can be found in Figure S6 and Video S3.

Experiments on challenging long-term parkour tasks show that RSG is able to achieve reasonable inference and accurate execution of skills in a large number of fundamental skills. Robots equipped with RSG have rich and diverse movement skills, and can smoothly and stably transition between different flexible behaviors, thereby quickly responding to complex and diverse unstructured terrain.

4.4 Skill Composition and Fast Learning

Humans or animals can learn new skills quickly from a few attempts at existing behaviors rather than starting from scratch. This rapid learning ability to solve new tasks or adapt to new environments is a key part of robot decision-making intelligence. Therefore, we set up three sets of experiments in simulation and reality to comprehensively analyze the rapid learning and adaptability of the proposed RSG.

In the first set of experiments (Fig. 5b), we consider how a robot can quickly learn a flexible and highly dynamic new skill, i.e., *Jump to Form a Circle (JFC)*. According to the requirements of the new skill *JFC*, the RSG performs skill inference through querying the related tasks and environments and obtains the three most matching fundamental skills: *Jump in Place (JP) Indoor Floor*, *Jump Left (JL) Indoor Floor*, and *Jump Backward (JB) Indoor Floor* skills (Fig. 5a). These three fundamental skills between low (0.7) and high (0.8) skill inference score thresholds will be utilized to learn new skills through Bayesian Optimization (BO) composition. Specifically, according to the distribution of skill inference scores, the tasks most relevant to new skills are *JP*, *JL*, and *JB*, followed by *Sidestep Left*, *Backward Left*, *Backward Walking*, etc. The most relevant environment is *Indoor Floor*, followed by *Steps*, *Grassland*, *Marble Slope Uphill*, etc. Furthermore, RSG takes into account both environmental similarity and task similarity when conducting skill inference. For example, for the fundamental skills *Sidestep Left Indoor Floor*, *Backward Left Indoor Floor*, *JP Upstairs* and *JP Grass and Sand*, they are only highly matched to the task (or environment), which results in a low final skill inference score (The environment for fundamental skills without specifications is *Indoor Floor*, the same applies hereafter). Intuitively, the reasoning behind RSG inference is aligned with human intuition. The essential attributes of the new skill *JFC* can be implicitly encoded through the skills *JP*, *JL*, and *JB* and achieved by jointly compositing them together. This assertion is also substantiated by the results presented in Fig. 5d, where the composition using BO achieves performance levels similar to the PPO algorithm when trained from scratch. The initial weights for the BO were determined by the skill inference scores obtained from RSG. This approach has been confirmed to facilitate the robot’s ‘warm boot’ as illustrated (Fig. 5d). This suggests that RSG not only accurately identifies the most relevant skills but also quantifies the relationship between the new skill and existing ones rationally. This attribute is of utmost significance for the robot’s bodily-kinesthetic intelligence, as it establishes a strong foundational basis for skill enhancement, ensuring stable and effective rapid learning and dynamic adaptation. Figure 5c clearly depicts the changing trends of biases and weights during BO composition. The biases corresponding to the three joints of the



■ Slope Ang = 10° ■ Slope Ang = 20° ■ Slope Ang = 30°

— Sidestep Left Walking Skill — Standing Skill

■ Baseline ■ Standing Skill ■ Composed Skill

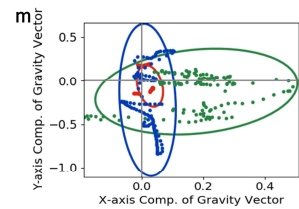
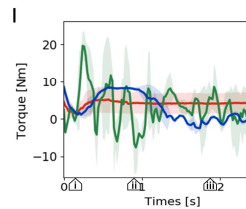
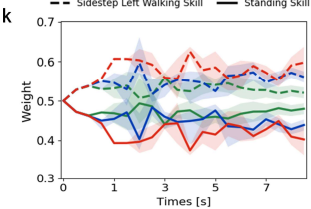


Fig. 5 | Rapid learning of new robot skills. **a**, Distribution of fundamental skills inference scores (greater than 0.3) in RSG corresponding to **b**. ‘/’ and ‘\’ type shading indicate the degree of matching with the tasks and the environments. The two black dashed horizontal lines represent high (0.9) and low (0.7) skill matching thresholds respectively. **b**, The fast learning process of new skill in simulation (*Jump to Form a Circle (JFC)*). The *jump left (JL)*, *jump backward (JB)*, and *jump in place (JP)* skills are selected for the *JFC* skill. **c**, The changing trends of biases and weights of BO corresponding to fundamental skills (right hind leg) of **b**. The shaded parts indicate the changing trends of other legs. **d**, Performance comparison with baseline. ‘Skill Reuse’ means directly utilizing the appropriate first skill inferred by RSG. ‘Random Init.’ indicates that the initial value of the corresponding BO weight of the fundamental skills is randomly sampled. ‘BO Comp.’ indicates that the normalized score of fundamental skills obtained by RSG skill inference is utilized as the initial BO weight. Three random seeds are used. **e**, The novel realistic quadrupedal gait rapid learning processes. The fundamental skill gaits obtained through RSG skill inference are *trot* and *crawl*. **f**, The changing trends of biases and weights of BO corresponding to fundamental skills (left hind leg) of **e**. The shaded parts indicate the changing trends of the other legs. **g**, Newly composited skill gaits corresponding to **e**. Gait patterns are represented by the touchdown state of the robot’s four legs. The shaded part indicates the gait of the fundamental skills. ‘/’ and ‘\’ represent *trot* and *crawl*. LF, left front leg; RF, right front leg; LH, left hind leg; RH, right hind leg. **h**, The joint position of the left hind leg in one cycle. **i**, The rapid adaptation process of the robot in the new environment (i.e. maintaining balance on slopes tasks). Two fundamental skills are utilized in RSG, the *standing* and *sidestep left walking* (or *sidestep right walking*) skills. **j**, Performance comparison with baseline methods. **k**, The variation trend of BO weight under different slopes. The shaded area represents the one standard deviation of triplicate experiments. **l-m**, Comparison of the trend of torque (front right calf) and comparison of the projections of gravity vectors on the horizontal plane corresponding to **j**. The ellipse represents 2.5 standard deviations. The experiment was repeated three times.

right hind leg finally converged to the range of -0.05 and 0.05, while the weights of the three fundamental skills finally converged to approximately 0.42, 0.38, and 0.22. A discrete point on each trajectory represents a BO iteration. Therefore, for the learning of new highly dynamic skills, the BO can converge using only about 20 optimization iterations. Essentially, the new skill is a linear transformation of the fundamental skills. The BO plays a role in the scalability of the action space of the DRL policy corresponding to the fundamental skills, so it can quickly iterate to convergence. Meanwhile, because linear composition is utilized, the extracted fundamental skills and the new skill have higher rationality and similarity. This also highlights that RSG’s skill inference based on entity relationships has better stability and interpretability. More results can be found in Video S4.

The practical movements of robots will inevitably lead them into scenarios and tasks that fall outside the scope of their training data. Therefore, a need for a variety of gaits will persist. Simultaneously, a robot’s ability to autonomously and efficiently generate new gaits in real-time equips it with a more adaptable and flexible locomotion

repertoire, enhancing its ability to cope with diverse environmental conditions. In the second set of experiments, we leveraged the fundamental skill gaits in RSG to rapidly composite novel gaits, as depicted in Fig. 5e. Figures 5f-h illustrate the evolving trends of biases and weights, the pattern of the newly acquired gait, and the joint position trajectory of the left hind leg. Over time, the biases for the three joints of the left hind leg converged to approximately 0.01, 0.02, and -0.01, while the weights for the two foundational skills, *Trot* and *Crawl*, eventually settled at around 0.58 and 0.42 (Fig. 5f). Fig. 5g vividly portrays the characteristics of the newly developed gait pattern, highlighting both its commonalities and distinctions from the fundamental skill gait pattern. The BO primarily acts as a linear transformation on the fundamental skill gait, predominantly influencing gait amplitude and, to some extent, gait frequency (as evident in Fig. 5h). For more detailed results, please refer to Video S5.

To verify the rapid adaptability of RSG-equipped robots to new environments, in the third set of experiments we compared several methods of maintaining balance in various slope environments (Fig. 5i). Figure 5k illustrates the changing trend of BO weight on different slopes. As the slope increases, the weight of the fundamental skill *standing* becomes smaller, while the weight of the fundamental skill *sidestep left walking* becomes larger. This is because the steeper the slope, the greater the friction the robot needs to compensate for the component of its gravity along the slope. This shows that the BO in RSG can adjust the weight of fundamental skills according to the characteristics of the environment, thereby better adapting to the new environment. Moreover, the qualitative (Fig. 5j) and quantitative (Fig. 5l-m) comparison results show that steep slopes belong to new scenarios outside the training distribution. The baseline method's torque fluctuates wildly between -10 and 20Nm, with both the X and Y components of gravity exceeding 0.4. This indicates that the baseline method attempts to adjust the robot's behavior to maintain balance on steep slopes but fails. The Y-direction component of gravity in the *standing*-only method exceeds 0.5, which means that a single skill cannot complete the task of standing stably. Compared with these methods, the new skills of BO combination can obviously enable the robot to have the smallest body posture fluctuation range and the smoothest torque, thereby successfully maintaining balance on steep slopes. This demonstrates the effectiveness and necessity of incorporating new robotic skills in real-time through BO in RSG when facing some challenging real-world scenarios. The comparison with baseline methods can be found in Video S6.

Extensive experiments have shown that robots configured with RSG have rapid learning capabilities, which is an integral part of robot intelligence and autonomy. This means that the robot can quickly learn new skills based on the behaviors it has already mastered, so as to better adapt to new environments and tasks.

5 DISCUSSION

Lack of behavior generation and fast dynamic adaptation in the face of varied tasks and environments is one of the key challenges that hinder the rapid advance of the quadruped robot in the physical world. Our research is devoted to exploring the flexible and adaptive motion behavior of the quadruped robot, inspired by the biological mechanism

behind the legged animals, which is able to generate versatile locomotion from the existing fundamental skills, upon the variations in the task and environment. We unfold this issue by proposing a novel framework RSG that links the task and the environment with the motion skill and allows for the association of many different abilities based on their connections to the task and the environment. Our results demonstrate that the implicit relationships between various forms of locomotion can be captured and manipulated for few-shot generalization. As a result, it is possible to develop flexible and adaptive motion behavior by combining related motions from a wide range of core skills. This is significant for the robot to reach high levels of autonomy and intelligence, particularly when it is deployed in the wild.

Similar to the knowledge graph, our proposed RSG can pack the relationships between different skills, tasks, and environments based on prior knowledge, and provides an effective way to manage and understand the vast amount of information behind them. This gives the quadrupedal robot the ability to infer reasonable locomotion behaviors in accordance with the new task or environment by digging out the internal explicit relationship among various skills. Such capability outperforms the existing purely data-driven models that are challenging to implement logical reasoning. As a result, with the aid of RSG, the quadrupedal robot can quickly choose the appropriate skills for varied terrains and perform expected motion in accordance with given tasks.

Additionally, our method can achieve rapid skill composition and generalization, in the case that the target task or environment has never been encountered before. Specifically, this capability is established upon a two-stage process. First, skill inference from RSG can manipulate the implicit relationships between the existing setting and the new setting and therefore lays a solid foundation for skill composition. The deployment of BO then offers the additional advantages of fast online adaptation, such that the legged robot controlled by the composited skill can quickly react to the altered task and environment. This is essential for robots to operate in unforeseen situations and is prominent in autonomous task executions. Furthermore, in contrast to the common goal-conditioned approaches, our proposed method also presents superiority over its counterparts in few-shot generalization. Particularly, the current goal-condition techniques are usually limited to locomotion gait. More complicated and flexible motions, such as jumping, rolling, and standup, are beyond its framework. Such a gap is bridged by the proposed method and the results demonstrate that the agile and dynamic motor skills of the legged robot are obtained after several attempts.

The quadrupedal robot with our proposed RSG demonstrates the flexible motion ability in the simulation setting and is able to quickly and properly respond to external changes. When it comes to reality, the discrepancy between the simulation and the physical world may accumulate and thus result in performance degradation. Domain randomization is one of the effective manners to tackle the simulation-to-reality problem. Nevertheless, it is commonly designed for a specific task and may lose its power when adopted in skill composition. The proposed BO-based motion composition method updates the control output in real time, thus alleviating this issue to a certain extent. To achieve fast online adaptation, currently, the model utilized in BO is linear, which restricts its performance in optimization of the flexible locomotion, especially when transferring from the simulation to the physics. Since the scope of the current

work is aimed at leveraging RSG for skill inference and composition rather than fully solving the simulation-to-reality problem, we leave it to future work.

Though our method exhibits huge potential in skill inference and behavior adaptation, the query information has to be provided by humans in advance, due to a lack of exteroceptive sensing. Integrating external sensory systems, such as vision, into the current framework may significantly enhance quadrupedal robot autonomy and intelligence when robots are deployed in the physical world. Intuitively, visual feedback may contain rich environmental information and can be utilized to plan the trajectory for the next task. As a result, the robot is able to understand environmental changes and generate task trajectories accordingly, from which the robot is capable of autonomously completing skill inference and composition without requiring help from humans. In future work, therefore, we will be dedicated to pursuing fully autonomous motion behavior generation by utilizing RSG upon the exteroception. More recently, perceptual intelligence has emerged from foundation models built in the fields of computer vision or natural language processing, and the RSG we proposed mainly improves the decision-making intelligence of robots. Coupling research between the two to promote the general intelligence of robots is also a promising research direction.

6 MATERIALS AND METHODS

The construction and application of RSG are mainly divided into three stages, as shown in Fig. 6. Firstly, we collect a large number of fundamental skills, including locomotion skill types and more flexible skill types. Then, based on a variant of the KGE model, we establish the relationship among skill, environment, and task entities to form a skill graph. Finally, we calculate the matching degree between the new required skills and the existing fundamental skills in RSG and utilize this to perform skill inference, query, and combination to achieve rapid learning.

6.1 Fundamental Skill Collection

Collecting a large and diverse set of fundamental skills is the first step in building the RSG. To make the skill distribution sufficiently rich and diverse, we model the robot’s behavior in the specific environment and task as a Markov decision process and utilize DRL-based methods to obtain various control policies. The environment and tasks corresponding to the trained control policies will be utilized to construct fundamental skills. Therefore, environment and task design first need to be considered.

The environmental design of legged robots mainly needs to consider terrain traversability (63). Intuitively, from a discrete perspective, the terrain can be assigned to separate categories, with each category having assumed mechanical properties of the terrain. An instance of terrain classification may be the distinction of terrain traversability (64). We can also describe some terrain properties, assigning continuous values to the terrain, such as slope (65), step height (66, 67), or roughness (68,69). For continuous measurements, the terrain traversability can be based on thresholding the values. For example, terrain traversability can be determined by individually thresholding terrain

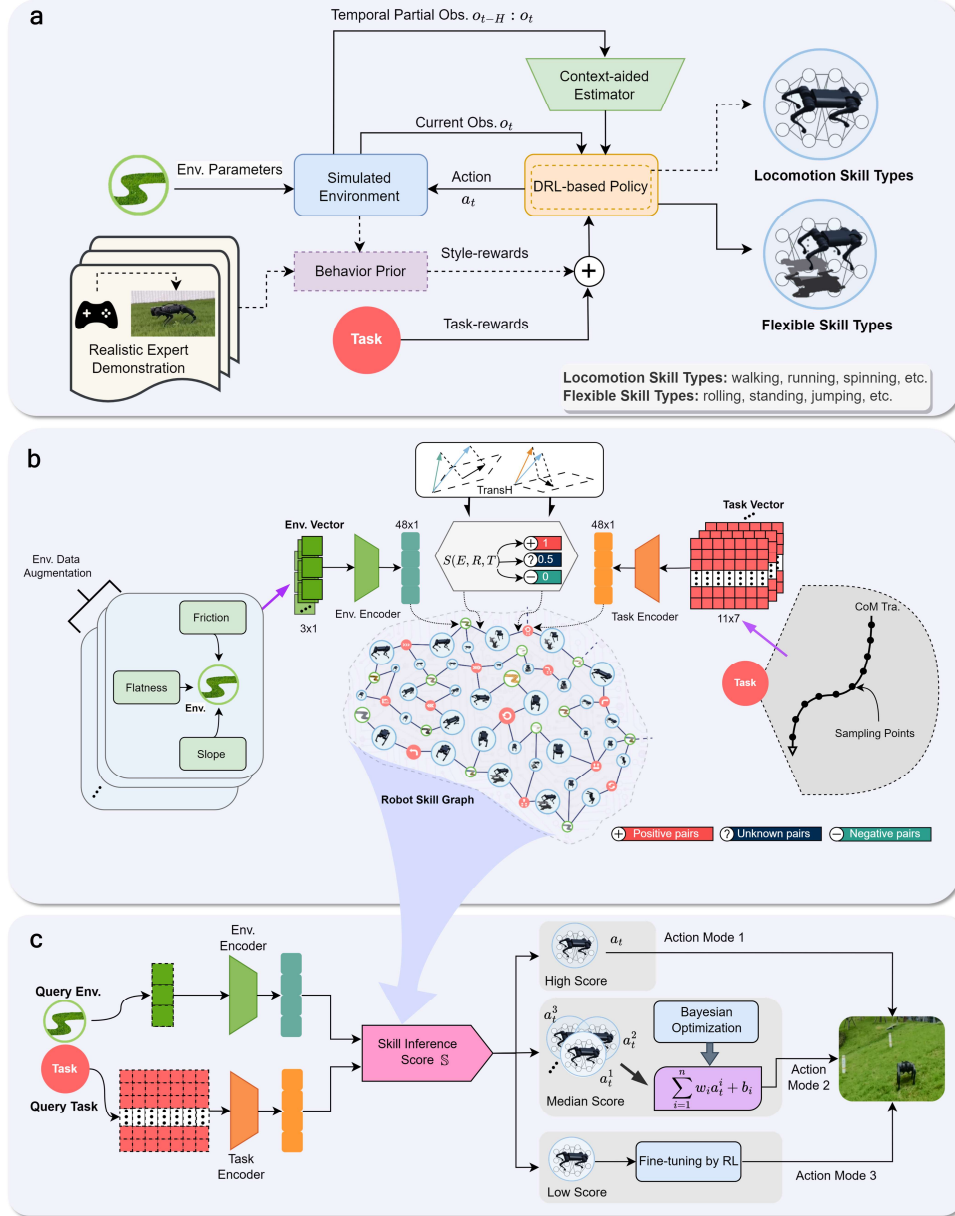


Fig. 6 | Overview of the presented RSG. a, Fundamental skills are divided into locomotion skill types (walking, running, spinning, etc.) and flexible skill types (rolling, standing, jumping, etc.). Both types of skills are trained using context-aided estimators to enhance the environmental representation. We also utilize adversarial motion priors to provide expert-style behavior for locomotion skill tasks. **b**, To construct the RSG, the environment is described as friction, flatness, and slope, and the task is

described as eleven consecutive CoM trajectory points. The environment and task descriptions are then mapped into latent variables respectively. A variant of the TransH method is leveraged to complete the relationship construction between skill entities, task entities, and environment entities. **c**, In the skill inference phase of RSG, given a new environment and task query, the score function is utilized to measure the match between the required new skills and the existing fundamental skills. For the final realistic application, according to the high, medium, and low scores of the selected skills, the action modes adopt the methods of skill reuse, BO composition, and RL fine-tuning respectively.

slope, roughness, and step height (65). Therefore, when building the simulated environment, we mainly consider the roughness, bumpiness, and steepness of the realistic terrain. All terrains in RSG are defined by three contact properties: friction, flatness, and slope. We construct various terrains based on the simulation platform IssacGym (70), where multiple environments run simultaneously on the GPU device to greatly accelerate the training process. Although the design of environmental attributes is straightforward, when training the control policy we will enhance the policy’s perception of the environment. The environment parameters are given in Table S1.

For task design, we consider common locomotion tasks and the more flexible behaviors of robots in the initial version of RSG. Locomotion tasks include relatively periodic horizontal movements on the horizontal plane, such as walking, running, spinning, etc. The main feature of this type of task is that the robot’s body remains basically parallel to the ground during its movement. More flexible behaviors are not limited to horizontal movements, such as jumping, rolling, standing (can return to a standing posture on unstructured ground or weird initial joint positions), etc. Its main characteristics are high dynamics, flexibility, and agility. In fact, any robot CoM trajectory can be used as a task type of RSG as long as the trajectory is available to the robot. In this way, during the deployment phase, as long as we specify a feasible CoM trajectory at will, the robot can immediately complete the corresponding complex behavior. More agile and dynamic, animal-like behavior will be built into RSG in the future.

For locomotion tasks, we first collect some expert demonstrations in reality by utilizing an off-the-shelf remote control to send velocity commands. These expert demonstrations could provide diverse periodic motion behaviors which is essential for developing skills with high quality. We adopt inverse reinforcement learning (IRL) to convert expert demonstrations into reward functions. Inspired by the adversarial motion priors (AMP) (71) method, a discriminator network is also utilized to distinguish expert demonstrations from policy-generated trajectories. The trained discriminator can be utilized as an intrinsic reward function for control policy training. The intrinsic reward function can guide the robot to learn a behavior style that is as close to the real expert demonstration as possible. Therefore, the total reward function is expressed:

$$r_t = w^g r_t^g + w^s r_t^s, \quad (1)$$

where r_t^g is the task-specific reward and r_t^s is the intrinsic reward generated by the AMP. w^g and w^s are hyperparameters. For more flexible behaviors, the reward

function is mainly defined manually without utilizing AMP. Moreover, the rolling and standing behaviors themselves are highly dynamic and intense. Simply relying on designing reward functions to smooth these behaviors is indirect and tricky (22). Therefore, we impose a penalty in the DRL training loss function to encourage gentle behavior $J = J_{DRL} + \hat{J}$. The additional regularization term \hat{J} is:

$$\hat{J} = \|\bar{q} - \mu(s_t)\|, \quad (2)$$

where the \bar{q} is the given joint position and the $\mu(s_t)$ is the action of the control policy (i.e. the desired joint position). The definitions of all tasks and related reward functions are given in Tables S2 and S3.

We utilize the classic model-free DRL algorithm, proximal policy optimization (PPO) (72), to train the control policy. For the implementation of PPO, an asymmetric actor-critic architecture is adopted (73). That is, the actor network only receives observations that are available in reality, while the critic network not only receives these observations but also receives privileged information that is difficult to measure in the real world. Besides, to strengthen environmental representations, we utilize a context-aided estimator network (CEN) (74). The CEN is inserted into the PPO training, which encodes the observation history over the past measurements to estimate the body velocity and implicitly infer the environmental representation. The CEN utilizes the historical data in the replay buffer of PPO for supervised training, and its labels are the linear velocity of the current time step and the observation of the next time step. Domain randomization techniques are also utilized to alleviate sim2real issues. More DRL training details can be found in Section S2. Hyperparameters are given in Tables S4 and S5.

6.2 RSG Construction

The RSG is constructed based on the framework of the KG. Normally, the KG consists of three components: entities, relations, and facts. In the RSG, entities include skills (s), environments (e), and tasks (t). We use context (c) to denote environment or task for brevity. Relations considered in our setting are environment to skill $r_{e \rightarrow s}$ and task to skill $r_{t \rightarrow s}$. Facts refer to all labeled triplets in the form of $(c, r_{c \rightarrow s}, s)$. The main challenge of representing robotics skills lies in how to jointly model prior information (e.g., the slope of environment, mechanic dynamics of robots) and implicit representation (meaning of skills, relations that link skill, and its corresponding context). In this paper, we construct a modified knowledge graph structure to tackle this issue.

The environments are represented by three properties: friction, flatness, and slope. We first define environment classes, where the properties of each environment class are not fixed values but a range. This is because when the control policy is trained in simulation, we adopt domain randomization technology. That is, the robot is trained in a certain range of environments with different physical properties. Moreover, environmental descriptions like “*grassland*” are actually vague. It could refer to various types of grass with different levels of friction and flatness. Therefore, during the construction

process of RSG, we sampled 100 instances from each environment class to characterize the environment.

To obtain an environment-agnostic task representation, we rollout the trained control policy 100 times in an anchor environment (*indoor floor*). Meanwhile, we collect seven key features of its motion trajectory as task representation:

$$\left(v_x^c, v_y^c, v_z^c, \|v^c\|, \mathbb{I}(\omega > 0), \mathbb{I}(\omega < 0), \|\omega\| \right), \quad (3)$$

where v_x^c, v_y^c and v_z^c are the normalized linear velocity components of the COM. $\|v^c\|$ is the norm of the linear velocity. $\mathbb{I}(\cdot)$ is indicator function and $\mathbb{I}(\omega \geq 0), \mathbb{I}(\omega < 0)$ are one-hot encoding representing the direction of yaw velocity. $\|\omega\|$ is the norm of the yaw angle velocity. In terms of skill and relationship representation, similar to the KGE, they are first initialized as random vectors and then iteratively optimized into reasonable representations. Subsequently, we build environment and task encoders, which are multilayer perceptrons. They are able to encode environment and task vectors into the same representation space as skills and relationships.

The key to training KGE is to construct positive and negative triples from all possible triples. Positive triples can be extracted directly from predefined labels since we know that the skill is trained in a certain environment and task. We then construct negative triples by constructing wrong-form triples, such as $(e, r_{e \rightarrow s}, e')$, $(t, r_{t \rightarrow s}, t')$, $(e, r_{t \rightarrow s}, s)$ and $(t, r_{e \rightarrow s}, s)$. We also construct soft triples, as triples with various plausibility. This is achieved by flipping the head entity in each positive triplet, such as $(e_{new}, r_{e \rightarrow s}, s_{original})$, and $(t_{new}, r_{t \rightarrow s}, s_{original})$. All these triples are fed into the scoring function. The scores of positive and negative samples are expected to be close to 1 and 0 respectively. The score of a soft triple is determined by margin ranking loss. This loss function is utilized to jointly train environment and task encoders, as well as skill and relation representations:

$$\mathcal{L} = \left(\mathbb{S}_{positive} - 1 \right)^2 + \left(\mathbb{S}_{negative} - 0 \right)^2 + \max(0, \mathbb{S}_{soft} - 1 + \delta), \quad (4)$$

where $\delta \propto \kappa(c_n, c_o)$ represents the margin and is determined by the similarity $\kappa(c_n, c_o)$ between the original context c_o and the new context c_n . Specifically, the similarity metric of environment representation is:

$$\kappa(e_n, e_o) = \max \left[\frac{|s_n - s_o|}{2}, \text{norm}(\|f_n - f_o, \delta_n - \delta_o\|) \right], \quad (5)$$

where f is the friction coefficient, δ is the flatness and s is the terrain slope. $\text{norm}(x) = x / x_{\max}$ represents normalization. The similarity metric of task representation is:

$$\kappa(t_n, t_o) = \max \left\{ \sum_t |sign(\omega_{n,t}) - sign(\omega_{o,t})|, \sum_t \left[1 - \left(\frac{v_{n,t}}{|v_{n,t}|} \right)^T \left(\frac{v_{o,t}}{|v_{o,t}|} \right) \right] \right\}, \quad (6)$$

where $\text{sign}(\bullet)$ represents sign function. The baseline KNN method used in context cross scores is introduced in Section S3. Moreover, we leverage the TransH model as the scoring function due to its ability to handle one-to-many and many-to-one relationships:

$$\mathbb{S}_{(h,r,t)} = e^{-\lambda \|(h-w_r^T h w_r) + d_r - (t-w_r^T t w_r)\|}, \quad (7)$$

where w_r and d_r are the norm and translation vector of the relationship, respectively. $\lambda=3$ is a hyperparameter. Readers can refer to the original paper (56) for other auxiliary losses in the TransH model.

6.3 Skill Inference and Composition

Skill inference tries to obtain the skills that are most likely to complete the given tasks and environments. At the inference time, the query environment and task vectors are first converted into embeddings with individual encoder. Then, the trained score function calculates the score between required skills and query entities. Effectively, we calculate $\mathbb{S}_{(t,r \rightarrow s)}^{\text{task}}$ and $\mathbb{S}_{(e,r \rightarrow s)}^{\text{env}}$ separately for all skills and multiply them together to obtain the final score:

$$\mathbb{S} = \mathbb{S}_{(t,r \rightarrow s)}^{\text{task}} \cdot \mathbb{S}_{(e,r \rightarrow s)}^{\text{env}}. \quad (8)$$

This score describes the matching degree that certain skills could be utilized in query context and on this basis, candidate fundamental skills in the RSG are extracted and returned. The asymptotic time complexity of skill inference is $O(cN)$, where c denotes number of contexts considered and N is the number of fundamental skills. Furthermore, skill composition studies how to generate the most proper skill for the query tasks and environments. Depending on the skill inference score, three different strategies are adopted.

When the score \mathbb{S} is high ($\alpha_{\text{high}} \leq \mathbb{S} \leq 1$), we directly utilize the skills returned by the RSG to solve the given tasks and environments. This is because entities similar to the query environments and tasks have already appeared in the RSG. The control policies corresponding to fundamental skills can be generalized to required tasks.

When the score \mathbb{S} is median ($\alpha_{\text{low}} \leq \mathbb{S} < \alpha_{\text{high}}$), all selected skills are composited by a parameterized linear model and then the parameters of such model are optimized through BO method. Considering that the learning of new skills has higher requirements for real-time and rapidity, compared with more complex skill composition methods, the BO is a better choice in terms of learning performance and efficiency (12). Assuming that the RSG in the skills inference phase has selected n skills, the linear combination can be expressed as:

$$a_t^* = \sum_{i=1}^n w_i a_t^i + b, \quad (9)$$

where the a_i^i is the action from the i^{th} fundamental skills. The weight w_i and bias b are the parameters of this linear model, and $\sum_{i=1}^n w_i = 1$. The score of selected fundamental skills by RSG inference is utilized as the initial value of weight optimization. All the parameters are optimized by BO so as to balance training speed and effectiveness. Essentially, the main function of the BO weight is to composite fundamental skills and establish links between foundation skills and newly learned skills. The main function of BO bias is to provide the ability to learn new skills to adapt quickly to new tasks (or environments). Furthermore, the reason why the BO method can be optimized in real time is that it performs the linear transformation on the action space of the control policy corresponding to the fundamental skills. This makes the action space of the skill more flexible, allowing it to adapt to the environment or tasks more quickly. More details can be found in Section S4.

When the score \mathbb{S} is low ($0 \leq \mathbb{S} < \alpha_{low}$), the selected fundamental skills will be fine-tuned by the DRL rather than learning from scratch. This situation arises because the query environment or task is out of distribution compared to the existing fundamental skills in RSG. The new skill obtained during the skill composition stage will be added to the RSG with its environment and task for RSG evolution and continuous learning. The expansion mechanism simulates the evolution in nature and the RSG will consist of more and more skills, environments, and tasks as usage increases. The RSG inference and composition process is given in Algorithm S1, and related hyperparameters are given in Table S6.

7 REFERENCES

1. Zhao, Feng, Ziqi Zhang, and Donglin Wang. KSG: Knowledge and Skill Graph [C]//Proceedings of the 31st ACM International Conference on Information & Knowledge Management. 2022: 4717-4721.
2. David Silver, Aja Huang, Chris J Maddison, Arthur Guez, Laurent Sifre, George Van Den Driessche, Julian Schrittwieser, Ioannis Antonoglou, Veda Panneershelvam, and Marc Lanctot. Mastering the game of go with deep neural networks and tree search. *nature*, 529(7587):484–489, 2016.
3. Silver, D., Hubert, T., Schrittwieser, J., Antonoglou, I., Lai, M., Guez, A., ... & Hassabis, D. (2018). A general reinforcement learning algorithm that masters chess, shogi, and Go through self-play. *Science*, 362(6419), 1140-1144.
4. Schrittwieser, J., Antonoglou, I., Hubert, T., Simonyan, K., Sifre, L., Schmitt, S., ... & Silver, D. (2020). Mastering atari, go, chess and shogi by planning with a learned model. *Nature*, 588(7839), 604-609.
5. Christopher Berner, Greg Brockman, Brooke Chan, Vicki Cheung, Przemyslaw Debiak, Christy Dennison, David Farhi, Quirin Fischer, Shariq Hashme, Christopher Hesse, Rafal Józefowicz, Scott Gray, Catherine Olsson, Jakub Pachocki, Michael Petrov, Henrique Pondé de Oliveira Pinto, Jonathan Raiman, Tim Salimans, Jeremy Schlatter, Jonas Schneider, Szymon Sidor, Ilya Sutskever, Jie Tang, Fi

- lip Wolski, and Susan Zhang. Dota 2 with large scale deep reinforcement learning. CoRR, abs/1912.06680, 2019. URL <http://arxiv.org/abs/1912.06680>.
6. Oriol Vinyals, Igor Babuschkin, Wojciech M. Czarnecki, Michaël Mathieu, Andrew Dudzik, Junyoung Chung, David H. Choi, Richard Powell, Timo Ewalds, Petko Georgiev, Junhyuk Oh, Dan Horgan, Manuel Kroiss, Ivo Danihelka, Aja Huang, Laurent Sifre, Trevor Cai, John P. Agapiou, Max Jaderberg, Alexander Sasha Vezhnevets, Rémi Leblond, Tobias Pohlen, Valentin Dalibard, David Budden, Yury Sulsky, James Molloy, Tom Le Paine, Çağlar Gülçehre, Ziyu Wang, Tobias Pfaff, Yuhuai Wu, Roman Ring, Dani Yogatama, Dario Wünsch, Katrina McKinney, Oliver Smith, Tom Schaul, Timothy P. Lillicrap, Koray Kavukcuoglu, Demis Hassabis, Chris Apps, and David Silver. Grandmaster level in starcraft II using multi-agent reinforcement learning. *Nat.*, 575(7782): 350–354, 2019. doi: 10.1038/s41586-019-1724-z. URL <https://doi.org/10.1038/s41586-019-1724-z>.
 7. Kun-Hsing Yu, Andrew L. Beam, and Isaac S. Kohane. Artificial intelligence in healthcare. *Nature Biomedical Engineering*, 2(10):719–731, October 2018. ISSN 2157- 846X. doi: 10.1038/s41551-018-0305-z. URL <https://www.nature.com/articles/s41551-018-0305-z>. Number: 10 Publisher: Nature Publishing Group.
 8. Choi, S., Ji, G., Park, J., Kim, H., Mun, J., Lee, J. H., & Hwangbo, J. (2023). Learning quadrupedal locomotion on deformable terrain. *Science Robotics*, 8(74), eade2256.
 9. Aditya Ramesh, Prafulla Dhariwal, Alex Nichol, Casey Chu, and Mark Chen. Hierarchical Text-Conditional Image Generation with CLIP Latents, April 2022. URL <http://arxiv.org/abs/2204.06125>. arXiv:2204.06125 [cs].
 10. Long Ouyang, Jeff Wu, Xu Jiang, Diogo Almeida, Carroll L. Wainwright, Pamela Mishkin, Chong Zhang, Sandhini Agarwal, Katarina Slama, Alex Ray, John Schulman, Jacob Hilton, Fraser Kelton, Luke Miller, Maddie Simens, Amanda Askell, Peter Welinder, Paul Christiano, Jan Leike, and Ryan Lowe. Training language models to follow instructions with human feedback[J]. *Advances in Neural Information Processing Systems*, 2022, 35: 27730-27744.
 11. Chitwan Saharia, William Chan, Saurabh Saxena, Lala Li, Jay Whang, Emily Denton, Seyed Kamyar Seyed Ghasemipour, Burcu Karagol Ayan, S. Sara Mahdavi, Rapha Gontijo Lopes, Tim Salimans, Jonathan Ho, David J. Fleet, and Mohammad Norouzi. Photorealistic Text-to-Image Diffusion Models with Deep Language Understanding[J]. *Advances in Neural Information Processing Systems*, 2022, 35: 36479-36494.
 12. Antoine Cully, Jeff Clune, Danesh Tarapore, and Jean-Baptiste Mouret. Robots that can adapt like animals. *Nature*, 521(7553):503–507, May 2015a. ISSN 1476-4687. doi: 10.1038/nature14422. URL <https://www.nature.com/articles/nature14422>. Number: 7553 Publisher: Nature Publishing Group.
 13. Carlson, Jennifer, and Robin R. Murphy. How UGVs physically fail in the field. *IEEE Transactions on Robotics*, 21(3):423–437, June 2005. ISSN 1941-0468. doi: 10.1109/TRO.2004.838027. Conference Name: IEEE Transactions on Robotics. Number: 7553 Publisher: Nature Publishing Group.

14. Dmitry Kalashnikov, Alex Irpan, Peter Pastor, Julian Ibarz, Alexander Herzog, Eric Jang, Deirdre Quillen, Ethan Holly, Mrinal Kalakrishnan, Vincent Vanhoucke, and Sergey Levine. Scalable deep reinforcement learning for vision-based robotic manipulation. In 2nd Annual Conference on Robot Learning, CoRL 2018, Zürich, Switzerland, 29-31 October 2018, Proceedings, volume 87 of Proceedings of Machine Learning Research, pp. 651–673. PMLR, 2018. URL <http://proceedings.mlr.press/v87/kalashnikov18a.html>
15. Frederik Ebert, Chelsea Finn, Sudeep Dasari, Annie Xie, Alex X. Lee, and Sergey Levine. Visual foresight: Model-based deep reinforcement learning for vision-based robotic control. CoRR, abs/1812.00568, 2018. URL <http://arxiv.org/abs/1812.00568>.
16. Nagabandi, A., Clavera, I., Liu, S., Fearing, R. S., Abbeel, P., Levine, S., & Finn, C. (2018). Learning to adapt in dynamic, real-world environments through meta-reinforcement learning. arXiv preprint arXiv:1803.11347.
17. Jinxin Liu, Hongyin Zhang, Zifeng Zhuang, Yachen Kang, Donglin Wang, and Bin Wang. (2023). Design from Policies: Conservative Test-Time Adaptation for Offline Policy Optimization. arXiv preprint arXiv:2306.14479.
18. Jemin Hwangbo, Joonho Lee, Alexey Dosovitskiy, Dario Bellicoso, Vassilios Tsounis, Vladlen Koltun, and Marco Hutter. Learning agile and dynamic motor skills for legged robots. *Science Robotics*, 4(26), 2019.
19. Joonho Lee, Jemin Hwangbo, Lorenz Wellhausen, Vladlen Koltun, and Marco Hutter. Learning quadrupedal locomotion over challenging terrain. *Science Robotics*, 5(47), 2020. doi: 10.1126/scirobotics.abc5986. URL <https://robotics.sciencemag.org/content/5/47/abc5986>.
20. Takahiro Miki, Joonho Lee, Jemin Hwangbo, Lorenz Wellhausen, Vladlen Koltun, and Marco Hutter. Learning robust perceptive locomotion for quadrupedal robots in the wild. *Science Robotics*, 7(62): eabk2822, 2022. doi: 10.1126/scirobotics.abk2822. URL <https://www.science.org/doi/abs/10.1126/scirobotics.abk2822>.
21. Lee, Joonho, Jemin Hwangbo, and Marco Hutter. Robust recovery controller for a quadrupedal robot using deep reinforcement learning[J]. arXiv preprint arXiv:1901.07517, 2019.
22. Chuanyu Yang, Kai Yuan, Qiuguo Zhu, Wanming Yu, and Zhibin Li. Multi-expert learning of adaptive legged locomotion. *Science Robotics*, 5(49):eabb2174, 2020.
23. Steven Bohez, Saran Tunyasuvunakool, Philemon Brakel, Fereshteh Sadeghi, Leonard Hasenclever, Yuval Tassa, Emilio Parisotto, Jan Humplik, Tuomas Haarnoja, and Roland Hafner. Imitate and repurpose: Learning reusable robot movement skills from human and animal behaviors. arXiv preprint arXiv:2203.17138, 2022.
24. Xiaoyu Huang, Zhongyu Li, Yanzhen Xiang, Yiming Ni, Yufeng Chi, Yunhao Li, Lizhi Yang, Xue Bin Peng, and Koushil Sreenath. Creating a dynamic quadrupedal robotic goalkeeper with reinforcement learning. arXiv preprint arXiv:2210.04435, 2022.
25. Abhik Singla, Shounak Bhattacharya, Dhaivat Dholakiya, Shalabh Bhatnagar, Ashitava Ghosal, Bharadwaj Amrutur, and Shishir Kolathaya. Realizing learned q

- quadruped locomotion behaviors through kinematic motion primitives. In International Conference on Robotics and Automation, ICRA 2019, Montreal, QC, Canada, May 20-24, 2019, pp. 7434–7440. IEEE, 2019. doi: 10.1109/ICRA.2019.8794179. URL <https://doi.org/10.1109/ICRA.2019.8794179>.
26. Xue Bin Peng, Erwin Coumans, Tingnan Zhang, Tsang-Wei Edward Lee, Jie Tan, and Sergey Levine. Learning agile robotic locomotion skills by imitating animals. In *Robotics: Science and Systems*, 07 2020. doi: 10.15607/RSS.2020.XVI.064.
 27. Eric Vollenweider, Marko Bjelonic, Victor Klemm, Nikita Rudin, Joonho Lee, and Marco Hutter. Advanced skills through multiple adversarial motion priors in reinforcement learning. *arXiv preprint arXiv:2203.14912*, 2022.
 28. Atil Iscen, Ken Caluwaerts, Jie Tan, Tingnan Zhang, Erwin Coumans, Vikas Sindhwani, and Vincent Vanhoucke. Policies modulating trajectory generators. In *2nd Annual Conference on Robot Learning, CoRL 2018, Zürich, Switzerland, 29-31 October 2018, Proceedings*, volume 87 of *Proceedings of Machine Learning Research*, pp. 916–926. PMLR, 2018. URL <http://proceedings.mlr.press/v87/iscen18a.html>.
 29. Deepali Jain, Atil Iscen, and Ken Caluwaerts. Hierarchical reinforcement learning for quadruped locomotion. In *2019 IEEE/RSJ International Conference on Intelligent Robots and Systems, IROS 2019, Macau, SAR, China, November 3-8, 2019*, pp. 7551–7557. IEEE, 2019. doi: 10.1109/IROS40897.2019.8967913. URL <https://doi.org/10.1109/IROS40897.2019.8967913>.
 30. Maurice Rahme, Ian Abraham, Matthew L. Elwin, and Todd D. Murphey. Dynamics and domain randomized gait modulation with bezier curves for sim-to-real legged locomotion. *CoRR*, abs/2010.12070, 2020. URL <https://arxiv.org/abs/2010.12070>.
 31. Hongyin Zhang, Jilong Wang, Zhengqing Wu, Yinuo Wang, and Donglin Wang. Terrain-aware risk-assessment-network-aided deep reinforcement learning for quadrupedal locomotion in tough terrain. In *IEEE/RSJ International Conference on Intelligent Robots and Systems, IROS 2021, Prague, Czech Republic, September 27 - Oct. 1, 2021*, pp. 4538–4545. IEEE, 2021. doi: 10.1109/IROS51168.2021.9636519. URL <https://doi.org/10.1109/IROS51168.2021.9636519>.
 32. Yuxiang Yang, Tingnan Zhang, Erwin Coumans, Jie Tan, and Byron Boots. Fast and efficient locomotion via learned gait transitions. In Aleksandra Faust, David Hsu, and Gerhard Neumann (eds.), *Conference on Robot Learning*, 8-11 November 2021, London, UK, volume 164 of *Proceedings of Machine Learning Research*, pp. 773–783. PMLR, 2021. URL <https://proceedings.mlr.press/v164/young22d.html>.
 33. Shangke Lyu, Han Zhao, Donglin Wang, A Composite Control Strategy for Quadruped Robot by Integrating Reinforcement Learning and Model-Based Control. *IEEE/RSJ International Conference on Intelligent Robots and Systems (IROS)*, 2023.
 34. Qingfeng Yao, Jilong Wang, Donglin Wang, Shuyu Yang, Hongyin Zhang, Yinuo Wang, and Zhengqing Wu. Hierarchical terrain-aware control for quadrupedal locomotion by combining deep reinforcement learning and optimal control. In *IE*

- EE/RSJ International Conference on Intelligent Robots and Systems, IROS 2021, Prague, Czech Republic, September 27 - Oct. 1, 2021, pp. 4546–4551. IEEE, 2021. doi: 10.1109/IROS51168.2021.9636738. URL <https://doi.org/10.1109/IROS51168.2021.9636738>.
35. Peng, X. B., Abbeel, P., Levine, S., & Van de Panne, M. (2018). Deepmimic: Example-guided deep reinforcement learning of physics-based character skills. *ACM Transactions On Graphics (TOG)*, 37(4), 1-14.
 36. Peng, X. B., Guo, Y., Halper, L., Levine, S., & Fidler, S. (2022). Ase: Large-scale reusable adversarial skill embeddings for physically simulated characters. *ACM Transactions On Graphics (TOG)*, 41(4), 1-17.
 37. Peng, X. B., Ma, Z., Abbeel, P., Levine, S., & Kanazawa, A. (2021). Amp: Adversarial motion priors for stylized physics-based character control. *ACM Transactions on Graphics (ToG)*, 40(4), 1-20.
 38. Richard S. Sutton, Doina Precup, and Satinder Singh. Between mdps and semi-mdps: A framework for temporal abstraction in reinforcement learning. *Artif. Intell.*, 112(1-2):181–211, 1999. doi: 10.1016/S0004-3702(99)00052-1. URL [https://doi.org/10.1016/S0004-3702\(99\)00052-1](https://doi.org/10.1016/S0004-3702(99)00052-1).
 39. Tanmay Shankar and Abhinav Gupta. Learning robot skills with temporal variational inference. In *Proceedings of the 37th International Conference on Machine Learning, ICML 2020, 13-18 July 2020, Virtual Event, volume 119 of Proceedings of Machine Learning Research*, pp. 8624–8633. PMLR, 2020. URL <http://proceedings.mlr.press/v119/shankar20b.html>.
 40. Tanmay Shankar, Yixin Lin, Aravind Rajeswaran, Vikash Kumar, Stuart Anderson, and Jean Oh. Translating robot skills: Learning unsupervised skill correspondences across robots. In Kamalika Chaudhuri, Stefanie Jegelka, Le Song, Csaba Szepesvári, Gang Niu, and Sivan Sabato (eds.), *International Conference on Machine Learning, ICML 2022, 17-23 July 2022, Baltimore, Maryland, USA, volume 162 of Proceedings of Machine Learning Research*, pp. 19626–19644. PMLR, 2022. URL <https://proceedings.mlr.press/v162/shankar22a.html>.
 41. Peter Pastor, Heiko Hoffmann, Tamim Asfour, and Stefan Schaal. Learning and generalization of motor skills by learning from demonstration. In *2009 IEEE International Conference on Robotics and Automation, ICRA 2009, Kobe, Japan, May 12-17, 2009*, pp. 763–768. IEEE, 2009. doi: 10.1109/ROBOT.2009.5152385. URL <https://doi.org/10.1109/ROBOT.2009.5152385>.
 42. Karl Pertsch, Youngwoon Lee, and Joseph J. Lim. Accelerating reinforcement learning with learned skill priors. In Jens Kober, Fabio Ramos, and Claire J. Tomlin (eds.), *4th Conference on Robot Learning, CoRL 2020, 16-18 November 2020, Virtual Event / Cambridge, MA, USA, volume 155 of Proceedings of Machine Learning Research*, pp. 188–204. PMLR, 2020. URL <https://proceedings.mlr.press/v155/pertsch21a.html>.
 43. Sasha Salter, Kristian Hartikainen, Walter Goodwin, and Ingmar Posner. Priors, hierarchy, and information asymmetry for skill transfer in reinforcement learning. *CoRR*, abs/2201.08115, 2022. URL <https://arxiv.org/abs/2201.08115>.
 44. Dushyant Rao, Fereshteh Sadeghi, Leonard Hasenclever, Markus Wulfmeier, Martina Zambelli, Giulia Vezzani, Dhruva Tirumala, Yusuf Aytar, Josh Merel, Nic

- olas Heess, and Raia Hadsell. Learning transferable motor skills with hierarchical latent mixture policies. In The Tenth International Conference on Learning Representations, ICLR 2022, Virtual Event, April 25-29, 2022. OpenReview.net, 2022. URL <https://openreview.net/forum?id=qTHBE7E9iej>.
45. Karl Pertsch, Youngwoon Lee, Yue Wu, and Joseph J. Lim. Demonstration-guided reinforcement learning with learned skills. In Aleksandra Faust, David Hsu, and Gerhard Neumann (eds.), Conference on Robot Learning, 8-11 November 2021, London, UK, volume 164 of Proceedings of Machine Learning Research, pp. 729–739. PMLR, 2021. URL <https://proceedings.mlr.press/v164/pertsch22a.html>.
 46. Nam, T., Sun, S. H., Pertsch, K., Hwang, S. J., & Lim, J. J. (2022). Skill-based meta-reinforcement learning. arXiv preprint arXiv:2204.11828.
 47. Adeniji, A., Xie, A., & Abbeel, P. (2022). Skill-based reinforcement learning with intrinsic reward matching. arXiv preprint arXiv:2210.07426.
 48. Residual skill policies: Learning an adaptable skill-based action space for reinforcement learning for robotics. In Conference on Robot Learning (pp. 2095-2104). PMLR.
 49. Ofir Nachum, Haoran Tang, Xingyu Lu, Shixiang Gu, Honglak Lee, and Sergey Levine. Why does hierarchy (sometimes) work so well in reinforcement learning? CoRR, abs/1909.10618, 2019. URL <http://arxiv.org/abs/1909.10618>.
 50. Youngwoon Lee, Joseph J. Lim, Anima Anandkumar, and Yuke Zhu. Adversarial skill chaining for long-horizon robot manipulation via terminal state regularization. In Aleksandra Faust, David Hsu, and Gerhard Neumann (eds.), Conference on Robot Learning, 8-11 November 2021, London, UK, volume 164 of Proceedings of Machine Learning Research, pp. 406–416. PMLR, 2021. URL <https://proceedings.mlr.press/v164/lee22a.html>.
 51. Huang, X., Batra, D., Rai, A., & Szot, A. (2023). Skill Transformer: A Monolithic Policy for Mobile Manipulation. In Proceedings of the IEEE/CVF International Conference on Computer Vision (pp. 10852-10862).
 52. Lucy Xiaoyang Shi, Joseph J. Lim, and Youngwoon Lee. Skill-based model-based reinforcement learning. CoRR, abs/2207.07560, 2022. doi: 10.48550/arXiv.2207.07560. URL <https://doi.org/10.48550/arXiv.2207.07560>.
 53. Shaoxiong Ji, Shirui Pan, Erik Cambria, Pekka Marttinen, and Philip S. Yu. A Survey on Knowledge Graphs: Representation, Acquisition, and Applications. IEEE Transactions on Neural Networks and Learning Systems, 33(2):494–514, February 2022. ISSN 2162-2388. doi: 10.1109/TNNLS.2021.3070843. Conference Name: IEEE Transactions on Neural Networks and Learning Systems.
 54. Mehdi Ali, Max Berrendorf, Charles Tapley Hoyt, Laurent Vermue, Mikhail Galkin, Sahand Sharifzadeh, Asja Fischer, Volker Tresp, and Jens Lehmann. Bringing Light Into the Dark: A Large-scale Evaluation of Knowledge Graph Embedding Models Under a Unified Framework. IEEE Transactions on Pattern Analysis and Machine Intelligence, 44(12):8825–8845, December 2022. ISSN 0162-8828, 2160-9292, 1939-3539. doi: 10.1109/TPAMI.2021.3124805. URL <http://arxiv.org/abs/2006.13365>. arXiv:2006.13365 [cs, stat].

55. Antoine Bordes, Nicolas Usunier, Alberto Garcia-Duran, Jason Weston, and Oksana Yakhnenko. Translating Embeddings for Modeling Multi-relational Data. In *Advances in Neural Information Processing Systems*, volume 26. Curran Associates, Inc., 2013. URL <https://papers.nips.cc/paper/2013/hash/1cecc7a77928ca8133fa24680a88d2f9-Abstract.html>.
56. Zhen Wang, Jianwen Zhang, Jianlin Feng, and Zheng Chen. Knowledge Graph Embedding by Translating on Hyperplanes. *Proceedings of the AAAI Conference on Artificial Intelligence*, 28(1), June 2014. ISSN 2374-3468. doi: 10.1609/aaai.v28i1.8870. URL <https://ojs.aaai.org/index.php/AAAI/article/view/8870>. Number: 1.
57. Zhiqing Sun, Zhi-Hong Deng, Jian-Yun Nie, and Jian Tang. RotatE: Knowledge Graph Embedding by Relational Rotation in Complex Space, February 2019. URL <http://arxiv.org/abs/1902.10197>. arXiv:1902.10197 [cs, stat].
58. Feiyang Wang, Zhongbao Zhang, Li Sun, Junda Ye, and Yang Yan. DirIE: Knowledge Graph Embedding with Dirichlet Distribution. In *Proceedings of the ACM Web Conference 2022, WWW '22*, pp. 3082–3091, New York, NY, USA, April 2022. Association for Computing Machinery. ISBN 978-1-4503-9096-5. doi: 10.1145/3485447.3512028. URL <https://doi.org/10.1145/3485447.3512028>.
59. Vinyals, Oriol, Blundell, Charles, Lillicrap, Tim, Wierstra, Daan. Matching networks for one shot learning. In *Neural Information Processing Systems (NIPS)*, 2016.
60. Jake Snell, Kevin Swersky, and Richard Zemel. 2017. Prototypical Networks for Few-shot Learning. In *Neural Information Processing Systems (NIPS)*, 2017.
61. Finn, Chelsea, Pieter Abbeel, and Sergey Levine. Model-agnostic meta-learning for fast adaptation of deep networks[C]//International conference on machine learning. PMLR, 2017: 1126-1135.
62. Smith, L., Kew, J. C., Peng, X. B., Ha, S., Tan, J., & Levine, S. (2022, May). Legged robots that keep on learning: Fine-tuning locomotion policies in the real world. In *2022 International Conference on Robotics and Automation (ICRA)* (pp. 1593-1599). IEEE.
63. Haddeler, G., Chuah, M. Y. M., You, Y., Chan, J., Adiwahono, A. H., Yau, W. Y., & Chew, C. M. (2022). Traversability analysis with vision and terrain probing for safe legged robot navigation. *Frontiers in Robotics and AI*, 9, 887910.
64. Bradley, D. M., Chang, J. K., Silver, D., Powers, M., Herman, H., Rander, P., & Stentz, A. (2015, September). Scene understanding for a high-mobility walking robot. In *2015 IEEE/RSJ International Conference on Intelligent Robots and Systems (IROS)* (pp. 1144-1151). IEEE.
65. Stelzer, A., Hirschmüller, H., & Görner, M. (2012). Stereo-vision-based navigation of a six-legged walking robot in unknown rough terrain. *The International Journal of Robotics Research*, 31(4), 381-402.
66. Homberger, T., Bjelonic, M., Kottege, N., & Borges, P. V. (2017). Terrain-dependent control of hexapod robots using vision. In *2016 International Symposium on Experimental Robotics* (pp. 92-102). Springer International Publishing.
67. Wermelinger, M., Fankhauser, P., Diethelm, R., Krüsi, P., Siegwart, R., & Huttenlocher, M. (2016, October). Navigation planning for legged robots in challenging terrain.

- in. In 2016 IEEE/RSJ International Conference on Intelligent Robots and Systems (IROS) (pp. 1184-1189). IEEE.
68. Krüsi, P., Furgale, P., Bosse, M., & Siegwart, R. (2017). Driving on point clouds: Motion planning, trajectory optimization, and terrain assessment in generic nonplanar environments. *Journal of Field Robotics*, 34(5), 940-984.
 69. Belter, D., Wietrzykowski, J., & Skrzypczyński, P. (2019). Employing natural terrain semantics in motion planning for a multi-legged robot. *Journal of Intelligent & Robotic Systems*, 93, 723-743.
 70. Makoviychuk, V., Wawrzyniak, L., Guo, Y., Lu, M., Storey, K., Macklin, M., ... & State, G. (2021). Isaac gym: High performance gpu-based physics simulation for robot learning. *arXiv preprint arXiv:2108.10470*.
 71. Escontrela, A., Peng, X. B., Yu, W., Zhang, T., Iscen, A., Goldberg, K., & Abbeel, P. (2022, October). Adversarial motion priors make good substitutes for complex reward functions. In 2022 IEEE/RSJ International Conference on Intelligent Robots and Systems (IROS) (pp. 25-32). IEEE.
 72. Schulman, J., Wolski, F., Dhariwal, P., Radford, A., & Klimov, O. (2017). Proximal policy optimization algorithms. *arXiv preprint arXiv:1707.06347*.
 73. Rudin, N., Hoeller, D., Reist, P., & Hutter, M. (2022, January). Learning to walk in minutes using massively parallel deep reinforcement learning. In *Conference on Robot Learning* (pp. 91-100). PMLR.
 74. Made Aswin Nahrendra, I., Yu, B., & Myung, H. (2023). DreamWaQ: Learning Robust Quadrupedal Locomotion with Implicit Terrain Imagination via Deep Reinforcement Learning. *arXiv e-prints*, arXiv-2301.

SUPPLEMENTARY MATERIALS

Table of Contents

- Section S1. More visual analysis of RSG using t-SNE
- Section S2. Data collection details, observations, and reward functions
- Section S3. The KNN method used in context cross scores
- Section S4. Skill composition by using Bayesian optimization
- Figure S1. Environment cross scores by RSG of forward walking skill
- Figure S2. Task cross scores by RSG on grassland environment
- Figure S3. Environment cross scores by KNN of forward walking skill
- Figure S4. Task cross scores by KNN on grassland
- Figure S5. Two front feet positions corresponding to the realistic robot parkour
- Figure S6. The robot's body speed corresponding to the simulated robot parkour
- Table S1. Environment parameters
- Table S2. Name and definition of reward functions
- Table S3. Definition of tasks
- Table S4. Definition of robot parameters and domain randomization
- Table S5. Hyperparameters of the PPO algorithm
- Table S6. Hyperparameters of the RSG inference and composition
- Algorithm S1. RSG inference and composition
- Video S1. Real-machine deployment of (partial) fundamental skills in RSG
- Video S2. The deployment of RSG for realistic robot parkour
- Video S3. The deployment of RSG for simulated robot parkour
- Video S4. The novel skill composition process in simulation
- Video S5. The new gait composition process in reality
- Video S6. Comparison of the proposed BO methods with baselines

S1. More visual analysis of RSG using t-SNE

Fig. S1 shows that environment cross scores of *forward walking* in all possible environments. Fig. S2 shows task cross scores on *grassland* for all possible tasks. Similar results are found on other tasks or environments, which are omitted for the sake of brevity. The visualization results in Figures S1 and S2 show that the RSG outputs scores with the following two properties: **1)** Non-related contexts are usually scored close to zero while highly-related contexts are scored near one. **2)** The score ranges of different context clusters are separated by clearer boundaries, which means that RSG discovers semantic representations. Furthermore, the results in Figures S3 and S4 show that the context cross scores by using the KNN method usually lack semantic information and span more widely. The scores for self-context (the original context used to train the skills) are not always close to one, and the scores for obviously irrelevant contexts are not close to zero. Therefore, vanilla similarity-based methods do not utilize predefined labels and struggle to learn clearly separated representations.

S2. Data collection details, observations, and reward functions

The hardware platform used in this work is the *Unitree A1* quadrupedal robot, which has a built-in controller that can follow high-level motion commands. We used a joystick to send velocity commands and generate multiple expert trajectories in various realistic terrains. The expert trajectories consist of base linear velocity, base angular velocity, joint position, joint velocity, body height, and foot position relative to the body. These demonstrations provide diverse periodic motion behaviors that can guide control policy training. The data were collected every 0.02 s using the legged SDK from the *Unitree A1* robot. At each time step, the information of contact force sensors, IMU, and joint encoders are recorded.

We utilize an asymmetric actor-critic architecture for policy training. Actions are defined as desired joint positions of 12 actuators at 50 Hz. The desired joint angles were tracked using the PD controller at 200 Hz ($K_p = 28$ and $K_d = 0.7$). The observation space of the policy network includes projected gravity, joint positions, joint velocities, actions of the previous time step, body angular velocity, and body linear velocity on the XY axis. The input of the critic network contains the policy observation, height scan around the body, foot contact forces, foot contact states, foot-ground friction coefficients, payloads, proportional gains of the PD controller, and derivative gains of the PD controller.

Inspired by previous works (1-3), the task reward is a linear combination of these basic reward functions multiplied by the time step $\Delta t = 0.02s$. The notations used in Table S3 are summarized as follows: $\exp(\bullet)$ and $\text{var}(\bullet)$ are exponential and variance operators, respectively. $(\bullet)^{des}$ and $(\bullet)^{cmd}$ indicate the desired and commanded values, respectively. x , y , and z are defined on the robot's body frame, with x and z pointing forward and upward, respectively. $g, v_{xy}, \omega_{yaw}, \theta_{base}, p_{f,y,j}, p_{f,z,j}, v_{f,xy,j}$ and τ are the gravity vector projected into the robot's body frame, linear velocities in the xy plane, yaw angle velocity, body orientation, foot width, foot height, foot lateral velocity, and joint torque, respectively. a_t, a_{t-1} and a_{t-2} are the actions of the current time step t , the previous time step $t-1$ and the previous time step $t-2$ respectively. h_{base} and h_{target} respectively

represent the current body height and expected body height of the robot. $\mathbf{g}_{default} = [0, 0, -1]$ is the default gravity vector. $\mathbf{1}_{contact,j}$ denotes the contact state of the j^{th} leg. $t_{air,j}$ denotes the swing time of the j^{th} leg in the air. The desired contact states $C_j^{cmd}(\bullet)$ are defined in (3).

S3. The KNN method used in context cross scores

To compute context cross scores by KNN methods, we firstly calculate centroid of original context class, then compute the similarity of each new context instance to it:

$$\kappa(c_n, c_o) = \text{norm}_c \left(\left\| c_n - \overline{\text{class}(c_o)} \right\| \right), \quad (1)$$

where $\text{class}(\bullet)$ finds centroid of class. $\text{norm}_c(x) = x / x_{\max}$ and x_{\max} are computed over all samples.

S4. Skill composition by using Bayesian optimization

In this section, we describe how fundamental skills are composed by using the BO method. Without loss of generality, suppose two different fundamental skills are selected from the RSG. The actions of the corresponding control policy are Gaussian distribution, which can be expressed as:

$$A_1 \sim \mathcal{N}(\mu_1, \sigma_1), A_2 \sim \mathcal{N}(\mu_2, \sigma_2), \quad (2)$$

where μ_i and σ_i are the mean and standard deviation of the Gaussian distribution, respectively. The goal of skill composition is to find a linear combination of two skills:

$$A_{new} = k_1 A_1 + k_2 A_2 + b \sim \mathcal{N}\left(k_1 \mu_1 + k_2 \mu_2 + b, (k_1 \sigma_1)^2 + (k_2 \sigma_2)^2\right), \quad (3)$$

that can maximize the cumulative rewards on the new task or environment.

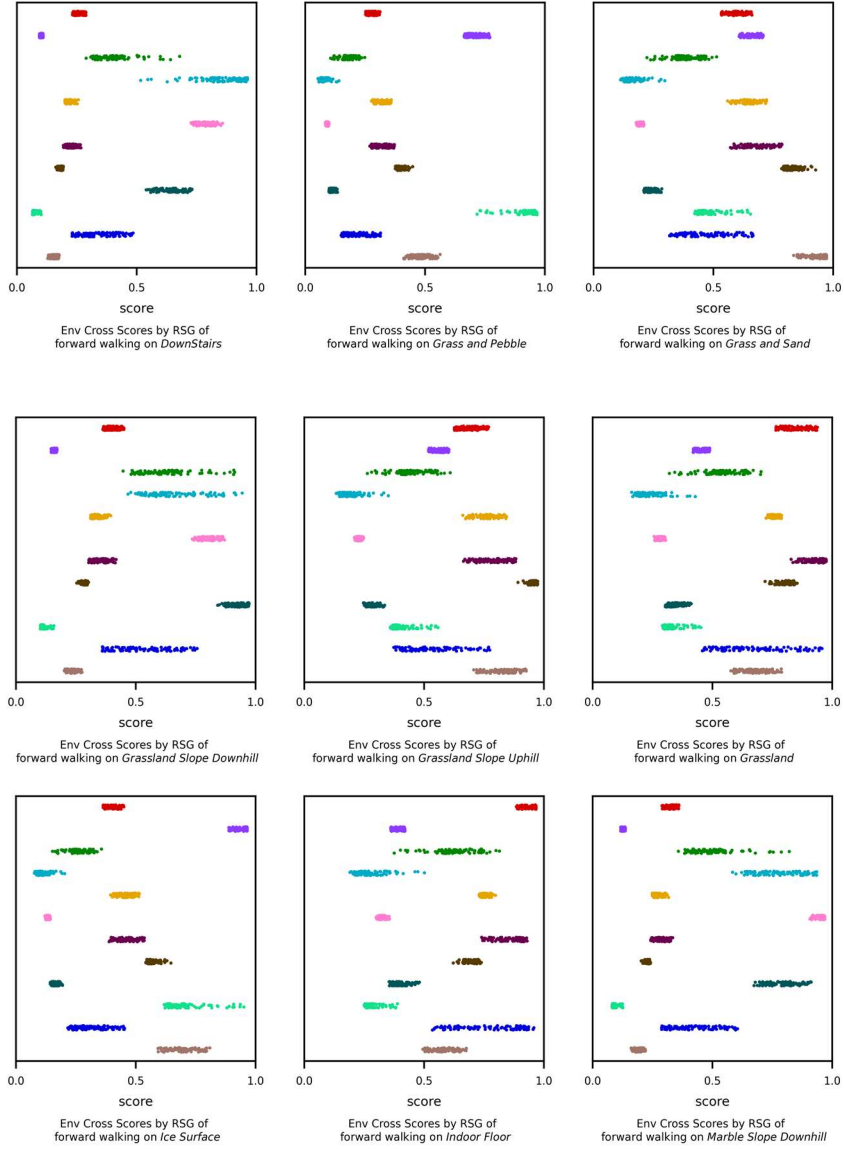
We utilized BO as the search method for the parameters $\mathbf{x} = [k_1, k_2, b]$. Assume that the observed return $y = f(\mathbf{x}) + \epsilon$ is an objective function of the parameters. $f(\mathbf{x})$ is described by a Gaussian Process (GP) model:

$$f(\mathbf{x}) \sim \mathcal{GP}(m(\mathbf{x}), k(\mathbf{x}, \mathbf{x}')), \quad (4)$$

where $m(\mathbf{x})$ and $k(\mathbf{x}, \mathbf{x}')$ are the mean function and kernel function, respectively. ϵ is the measurement noise of the returns, which is assumed to follow a normal distribution $\epsilon \sim \mathcal{N}(0, \sigma_{\text{noise}}^2)$, where σ_{noise}^2 is a hyperparameter. the mean function is a constant m_0 and the kernel function is selected as a Gaussian kernel:

$$k(\mathbf{x}, \mathbf{x}') = \sigma_f^2 \exp\left(-\frac{1}{2l^2} \|\mathbf{x} - \mathbf{x}'\|^2\right), \quad (5)$$

where σ_f and l are the hyperparameters of the kernel. The sampled parameters are stored in a dataset D and the GP model is iteratively updated to fit the dataset and find the optimal point \mathbf{x}^* .



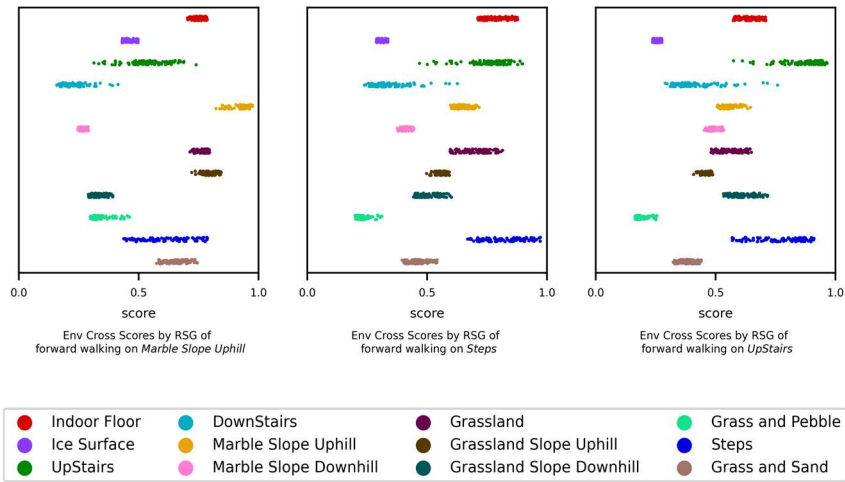
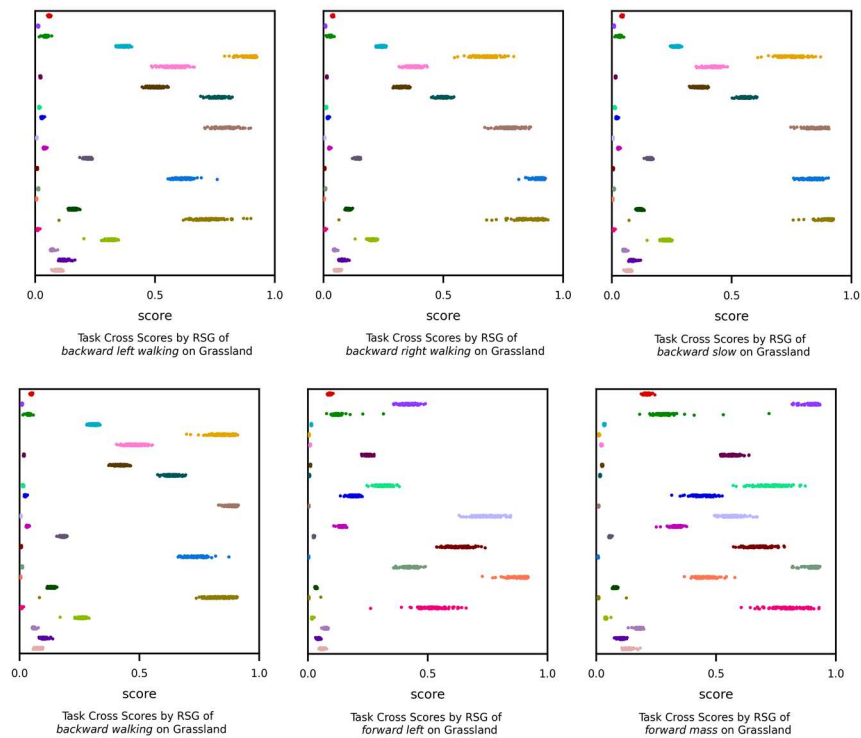
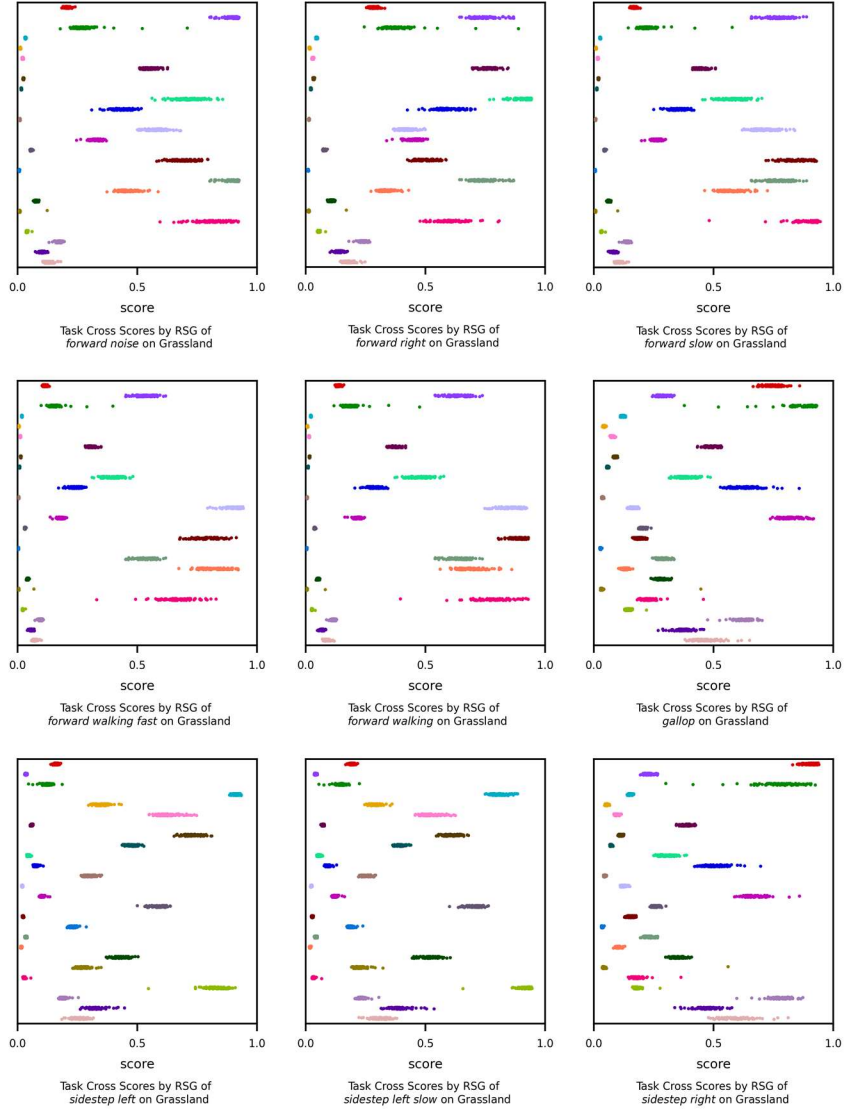
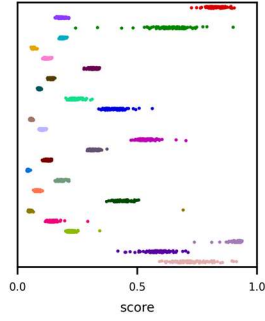


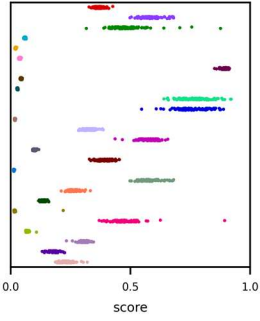
Fig. S1. Environment cross scores by RSG of forward walking skill.



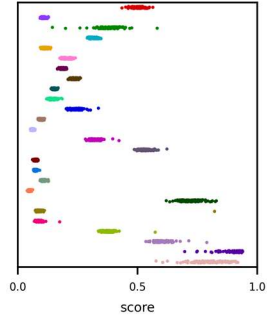




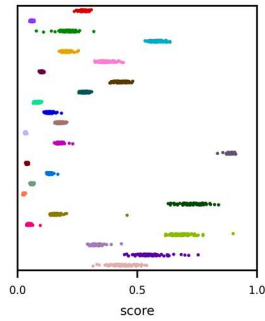
Task Cross Scores by RSG of
sidestep right slow on Grassland



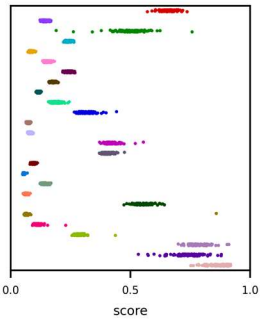
Task Cross Scores by RSG of
spin clockwise on Grassland



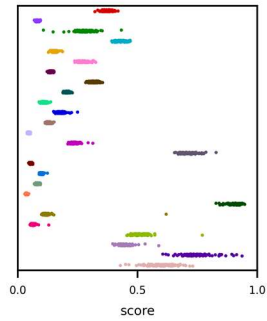
Task Cross Scores by RSG of
spin clockwise slow on Grassland



Task Cross Scores by RSG of
spin counterclockwise on Grassland



Task Cross Scores by RSG of
spin counterclockwise slow on Grassland



Task Cross Scores by RSG of
standup on Grassland

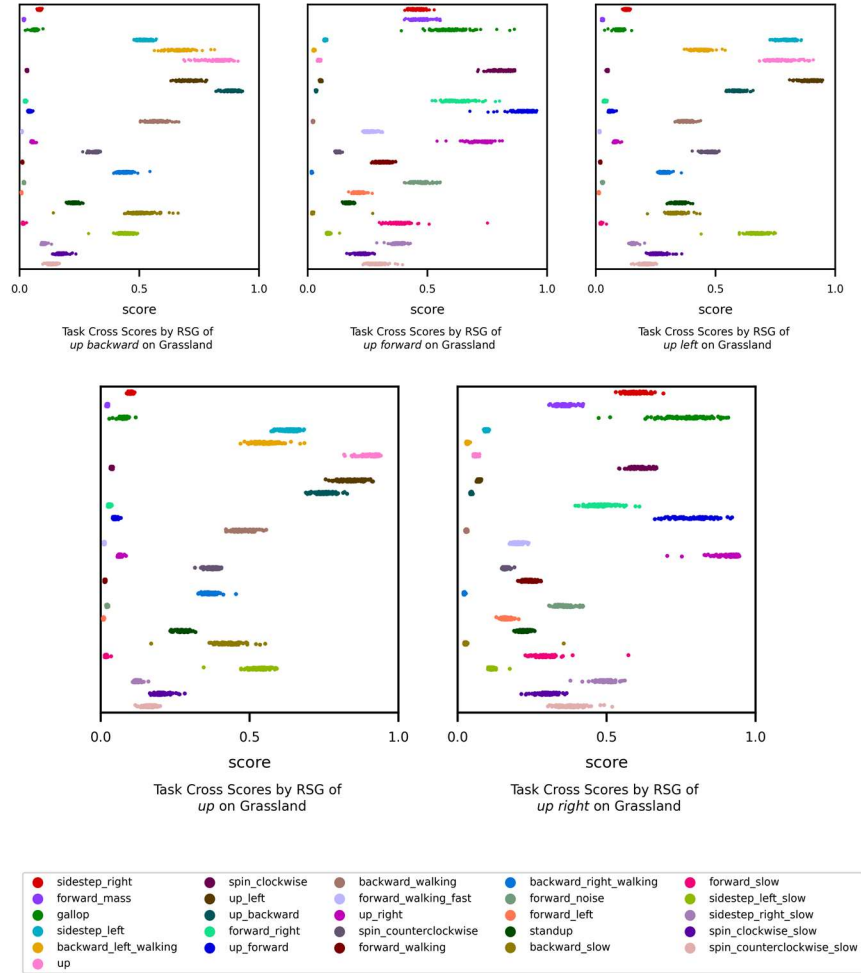
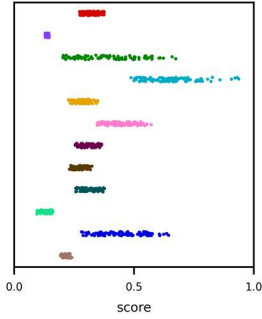
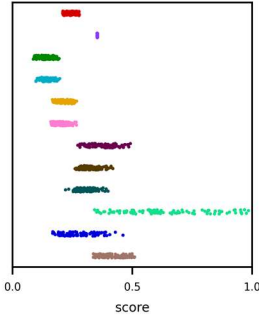


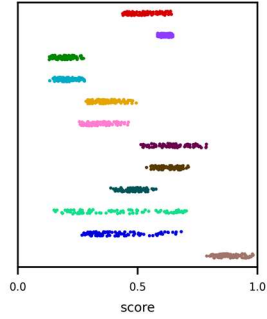
Fig. S2. Task cross scores by RSG on grassland environment.



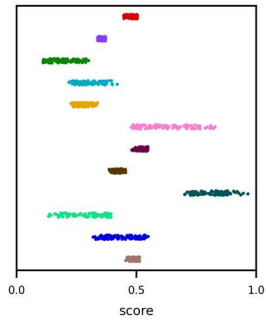
Env Cross Scores by KNN of forward walking on *DownStairs*



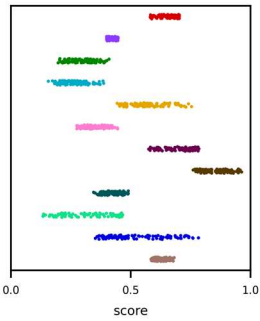
Env Cross Scores by KNN of forward walking on *Grass and Pebble*



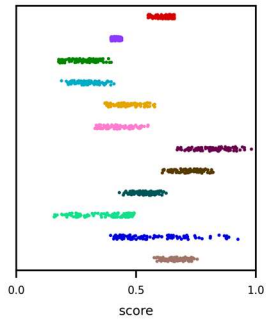
Env Cross Scores by KNN of forward walking on *Grass and Sand*



Env Cross Scores by KNN of forward walking on *Grassland Slope Downhill*



Env Cross Scores by KNN of forward walking on *Grassland Slope Uphill*



Env Cross Scores by KNN of forward walking on *Grassland*

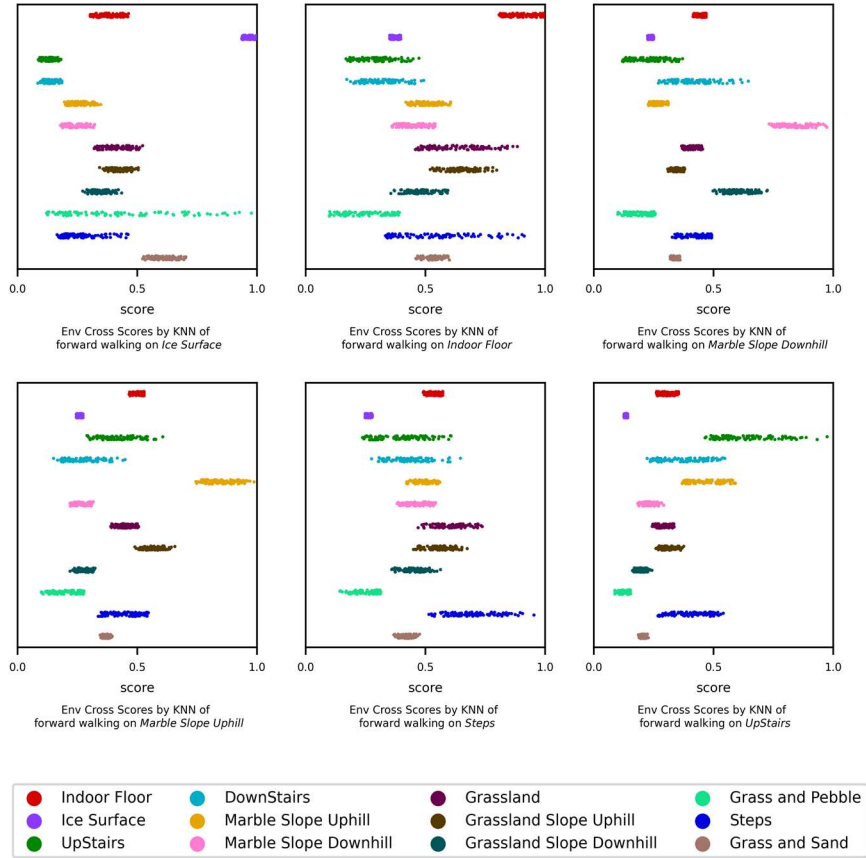
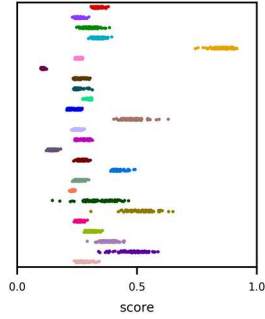
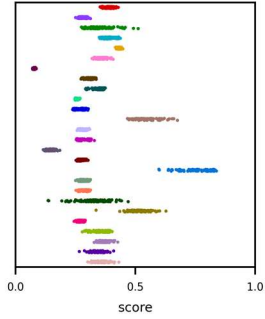


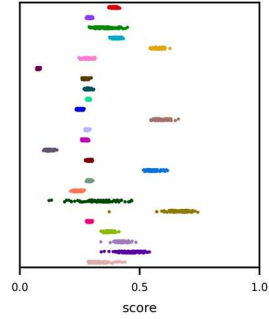
Fig. S3. Environment cross scores by KNN of *forward walking* skill.



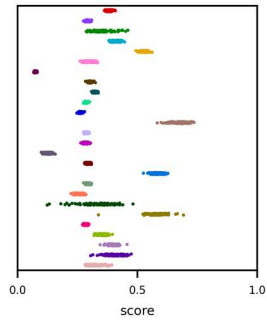
Task Cross Scores by KNN of
backward left walking on Grassland



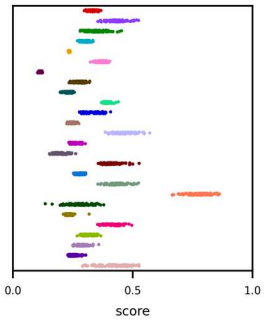
Task Cross Scores by KNN of
backward right walking on Grassland



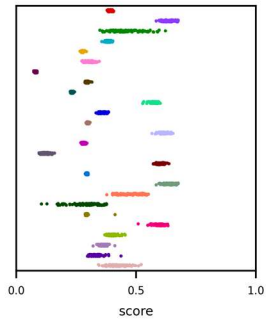
Task Cross Scores by KNN of
backward slow on Grassland



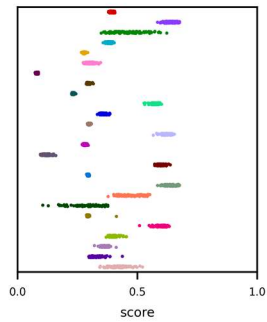
Task Cross Scores by KNN of
backward walking on Grassland



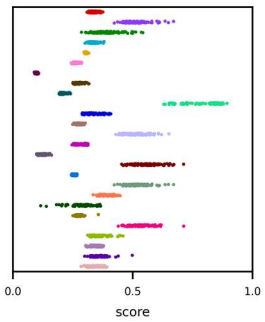
Task Cross Scores by KNN of
forward left on Grassland



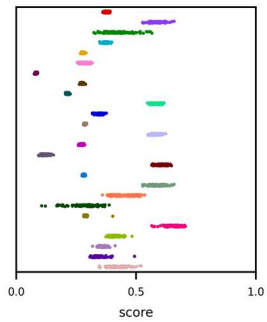
Task Cross Scores by KNN of
forward mass on Grassland



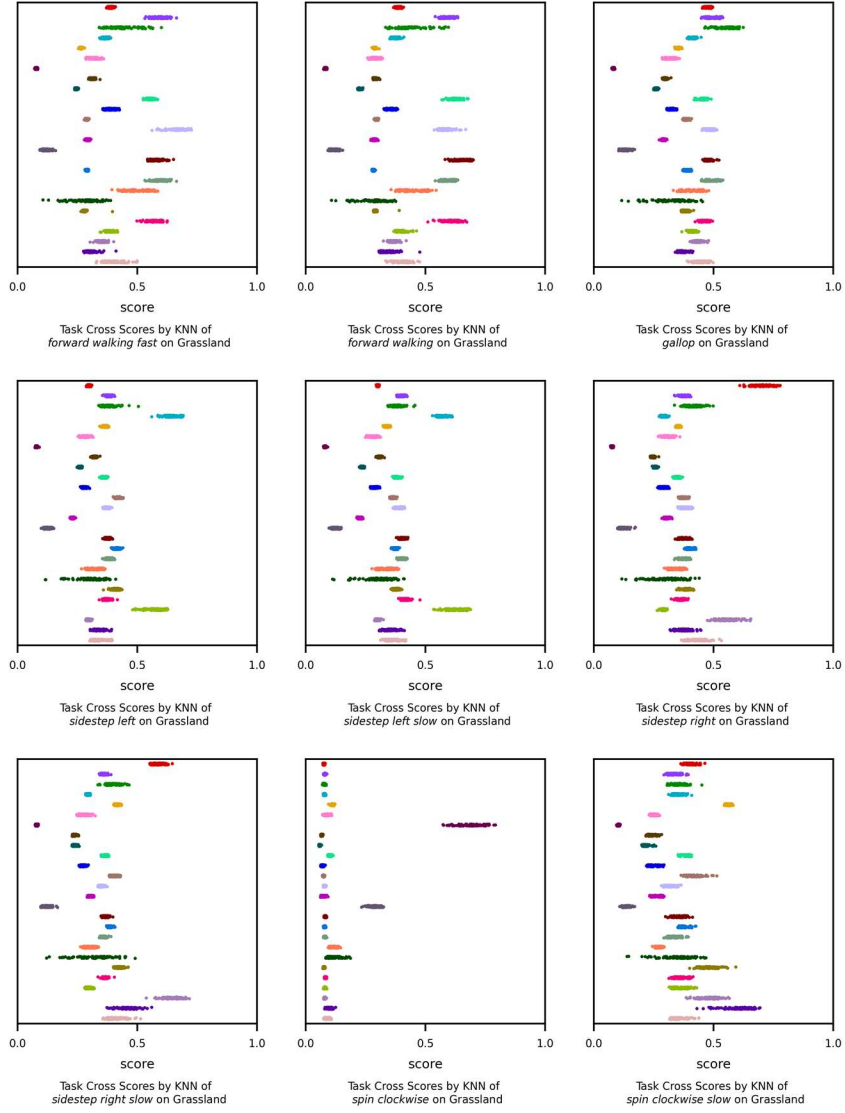
Task Cross Scores by KNN of
forward noise on Grassland



Task Cross Scores by KNN of
forward right on Grassland



Task Cross Scores by KNN of
forward slow on Grassland



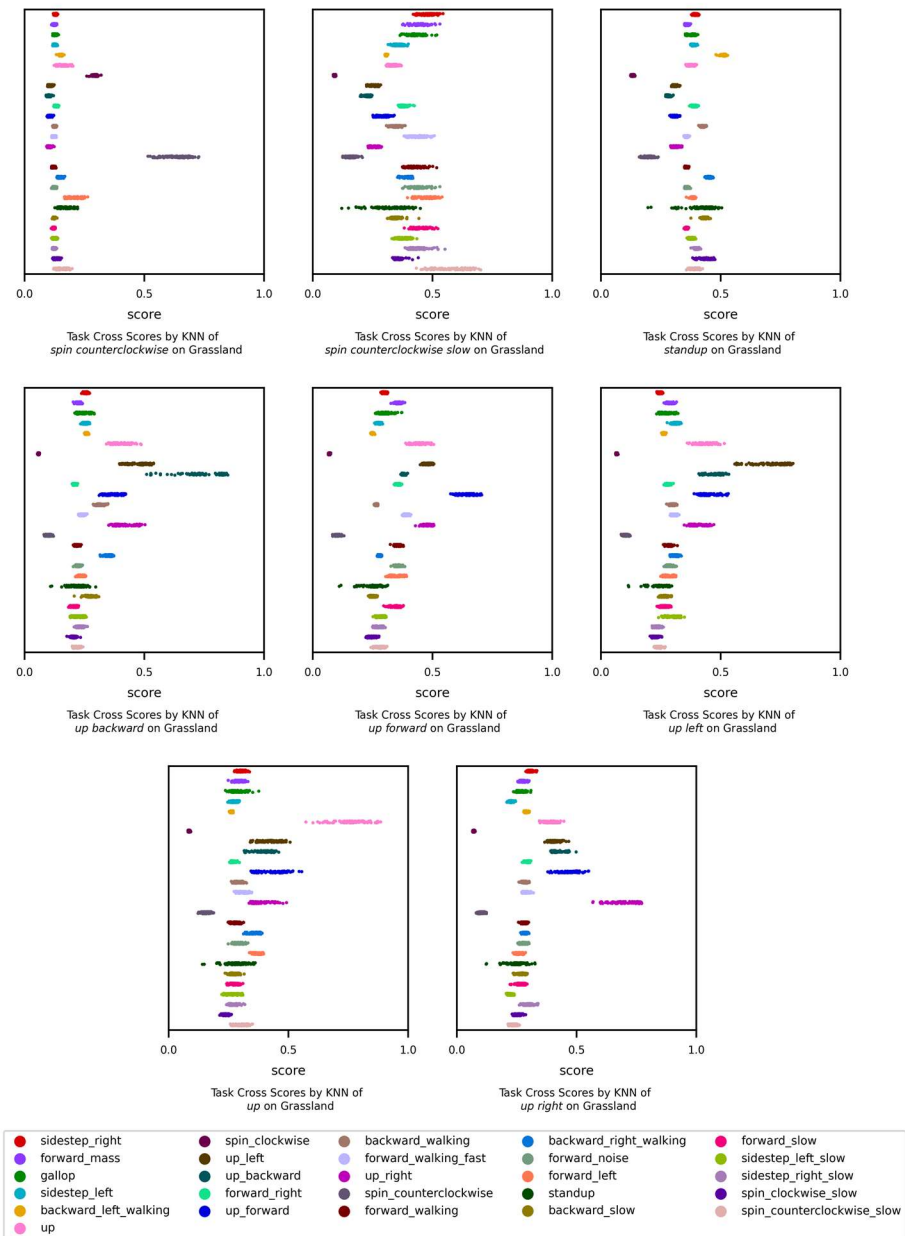


Fig. S4. Task cross scores by KNN on *grassland*

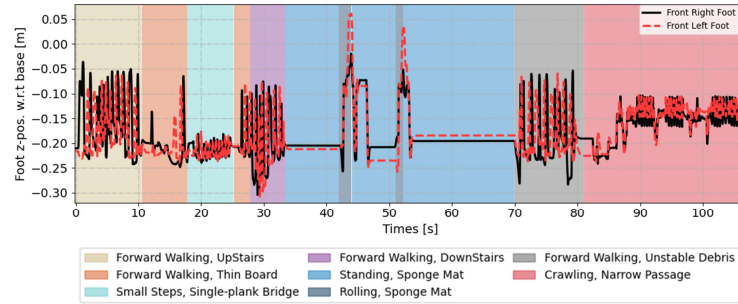


Fig. S5. The profiles of two front feet positions corresponding to the realistic robot parkour in Fig. 4a.

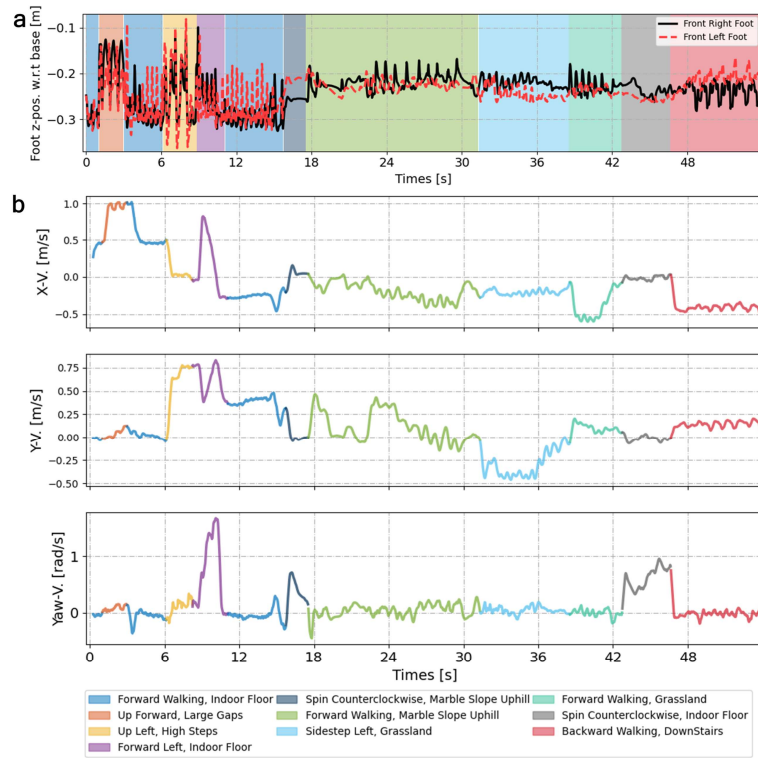


Fig. S6. The profiles of two front feet positions (a) and the robot's body speed (b) corresponding to the simulated robot parkour in Fig. 4f.

Tab. S1. Environment parameters.

Environment Name	Friction Range	Flatness Range	Slope Range
Indoor Floor	[0.6, 0.9]	0	0
Ice Surface	[0.01, 0.1]	0	0
Upstairs	[1.2, 1.5]	[0, 13.125]	[0, 0.4]
Downstairs	[1.2, 1.5]	[0, 14.375]	[-0.26, 0]
Marble Slope Uphill	[0.7, 1.1]	[2.25, 2.625]	[0.15, 0.25]
Marble Slope Downhill	[0.7, 1.1]	[3.0, 3.375]	[-0.3, 0.18]
Grassland	[0.5, 0.7]	[0.25, 9.0]	0
Grassland Slope Uphill	[0.5, 0.7]	[0.25, 6.125]	[0.06, 0.1]
Grassland Slope Downhill	[0.5, 0.7]	[0.375, 7.75]	[-0.25, 0.15]
Grass and Pebble	[0.05, 0.1]	[0, 25.375]	0
Steps	[0.6, 1.2]	[0, 12.75]	0
Grass and Sand	[0.3, 0.4]	[0.25, 5.625]	0

Tab. S2. Name and definition of reward functions.

Reward Name	Reward Definition
Linear Velocity Tracking (LVT)	$\exp\left(-\left(v_{xy} - v_{xy}^{cmd}\right)^2 / 0.25\right)$
Angular Velocity Tracking (AVT)	$\exp\left(-\left(\omega_{yaw} - \omega_{yaw}^{cmd}\right)^2 / 0.25\right)$
Torques Square (TS)	τ^2
Action Rate (AR)	$(a_{t-1} - a_t)^2$
Joint Acceleration (JA)	\dot{q}^2
Joint Power (JP)	$ \tau \dot{q} $
Base Height (BH)	$(h_{base} - h_{target})^2$
Feet Clearance (FC)	$\sum_{j=0}^4 \left[(h_{base} - p_{f,z,j}) - p_{f,z,j}^{des} \right]^2 \ v_{f,xy,j}\ _2$
Feet Air Time (FAT)	$\sum_{j=0}^4 (t_{air,j} - 0.5)$
Joint Power Distribution (JPD)	$\text{var}(\tau \dot{q})^2$
Linear Velocity Penalty (LVP)	v_z^2
Angular Velocity Penalty (AVP)	ω_{xy}^2

Body Orientation Penalty (BOP)	$ g ^2$
Joint Smoothness (JS)	$(a_t - 2a_{t-1} + a_{t-2})^2$
Lie Orientation (LO)	$\exp(- g_3 - g_{default,3} /0.25)$
Foot Full Contact (FFC)	$\sum_{j=1}^4 \mathbf{1}_{contact,j}$
Jump Position (JP)	$\begin{cases} \exp(- h_{base} - h_{target} /0.25)v_z, & \text{if } v_z > 0; \\ 0, & \text{otherwise.} \end{cases}$
Jump Body Height (JBH)	$\begin{cases} \exp(- h_{base,z} - h_{target,z} /0.25)v_z, & \text{if } v_z > 0; \\ 0, & \text{otherwise.} \end{cases}$
Lie Position (LP)	$\begin{cases} \exp(- q - q_{default,lie} /0.25), & \text{if } \theta_{roll} \leq 0.3; \\ 0, & \text{otherwise.} \end{cases}$
Base Uprightness (BU)	$1 - g_3$
Yaw Angle Velocity (YAV)	$\exp(- \omega_{yaw} /0.25)$
Stand Hip Position (SHP)	$\exp\left(-\sum_{i \in \{0,1,2,3\}} q_{3i+3} /0.25\right)$
Lie Orientation RPY (LORPY)	$\exp(- \theta_{base} /0.25)$
Feet Distance Penalty (FDP)	$\sum_{j=0}^4 p_{f,y,j} $
Foot Swing Height Tracking (FSHT)	$\sum_j (p_{f,z,j} - p_{f,z,j}^{cmd})^2 C_j^{cmd}(\theta^{cmd}, t)$

Tab. S3. Definition of tasks.

Task Name	Task Commands	Task Rewards	Use AMP?	Additional Information
Forward Walking	[0.6, 0, 0, 0, 0, 0]	5LVT + 1.5AVT - 10BH - 0.01TS - 1AR	Yes	
Forward Right	[0.4, 0, 0, 0, 0, -0.4]	5LVT + 1.5AVT - 0.01TS - 1AR	Yes	
Forward Left	[0.4, 0, 0, 0, 0, 0.4]	5LVT + 1.5AVT - 0.01TS - 1AR	Yes	
Backward Walking	[-0.6, 0, 0, 0, 0, 0]	5LVT + 1.5AVT - 0.01TS - 1AR	Yes	
Backward Right	[-0.5, 0, 0, 0, 0, 0.4]	5LVT + 1.5AVT - 0.01TS - 1AR	Yes	
Backward Left	[-0.4, 0, 0, 0, 0, 0.4]	5LVT + 1.5AVT - 0.01TS - 1AR	Yes	
Sidestep Right	[0, -0.6, 0, 0, 0, 0]	5LVT + 1.5AVT - 0.01TS - 1AR	Yes	

Sidestep Left	[0, 0.6, 0, 0, 0, 0]	5LVT + 1.5AVT - 0.01TS - 1AR	Yes	
Spin Clockwise	[0, 0, 0, 0, 0, -4]	1.5LVT + 5AVT - 0.01TS - 1AR	Yes	
Spin Counter- clockwise	[0, 0, 0, 0, 0, 4]	1.5LVT + 5AVT - 0.01TS - 1AR	Yes	
Gallop	[2, 0, 0, 0, 0, 0]	5LVT + 1.5AVT - 0.01TS - 1AR	Yes	
Forward Walking Fast	[1, 0, 0, 0, 0, 0]	5LVT + 1.5AVT - 0.01TS - 1AR	Yes	
Forward Mass	[0.6, 0, 0, 0, 0, 0]	5LVT + 1.5AVT - 0.01TS - 1AR	Yes	Robot base mass has twice the randomization range as other tasks
Forward Noise	[0.6, 0, 0, 0, 0, 0]	5LVT + 1.5AVT - 0.01TS - 1AR	Yes	Observation noise has twice the randomization range than other tasks
Jump in Place (up)	[0, 0, 2, 0, 0, 0, 0, 0, 0.6]	10JP - 10FFC + 10LO + 10 LORPY - 0.001TS - 0.1AR	No	$h_{target} = [0, 0, 0.6]$
Jump Backward (up back- ward)	[-1, 0, 2, 0, 0, 0, 0, 0, 0.6]	5LVT + 1.5AVT + 10JBH - 10FFC + 10LO + 10LORPY - 0.001TS - 0.1AR	No	$h_{target,z} = 0.6$
Jump For- ward (up forward)	[1, 0, 2, 0, 0, 0, 0, 0, 0.6]	5LVT + 1.5AVT + 10JBH - 10FFC + 10LO + 10LORPY - 0.001TS - 0.1AR	No	$h_{target,z} = 0.6$
Jump Left (up left)	[0, 0.75, 2, 0, 0, 0, 0, 0, 0.6]	5LVT + 1.5AVT + 10JBH - 10FFC + 10LO + 10LORPY - 0.001TS - 0.1AR	No	$h_{target,z} = 0.6$
Jump Right (up right)	[0, -0.75, 2, 0, 0, 0, 0, 0, 0.6]	5LVT + 1.5AVT + 10JBH - 10FFC + 10LO + 10LORPY - 0.001TS - 0.1AR	No	$h_{target,z} = 0.6$
Roll	[0, 0, 0, 0, 0, 0]	3LP+1BU+1FFC+2YAV-0.000001JA-0.00001JP-0.05AR	No	$q_{defab,lie} = [0., 1.56, -2.7, 0., 1.56, -2.7, 0., 1.56, -2.7, 0., 1.56, -2.7]$
Standup (standing)	[0, 0, 0, 0, 0, 0]	1SHP+1BU+1BH+1FFC-0.000001JA-0.00001JP-0.05AR	No	
Crawl	[0.3, 0, 0, 0, 0, 0]	1LVT+0.5AVT-1BH-1.5FC+1FAT-2LVP-0.2BOP-0.01AR-0.01AS-0.05AVP-0.00000025JA-0.00002JP-0.0000001JPD	No	$h_{target} = 0.15$ $p_{f,z,j}^{des} = 0.06$
Trot	[0.3, 0, 0, 0, 0, 0]	1LVT+0.5AVT-1BH-0.6FSHT+1FAT-2LVP-0.2BOP-0.01AR-0.01AS-0.05AVP-0.00000025JA-0.00002JP-0.0000001JPD	No	$\theta^{cmd} = (0.5, 0, 0)$

Pace	[0.3, 0, 0, 0, 0, 0]	1LVT+0.5AVT-1BH-0.6FSHT +1FAT-2LVP-0.2BOP-0.01AR- 0.01AS-0.05AVP-0.0000025JA- 0.00002JP-0.000001JPD	No	$\theta^{cmd} = (0., 0, 0.5)$
Small Steps	[0.3, 0, 0, 0, 0, 0]	1LVT+0.5AVT-1BH-1.5FC+1FAT- 2LVP-0.2BOP-0.01AR-0.01AS- 0.05AVP-0.0000025JA-0.00002JP- 0.000001JPD-0.5FDP	No	
Others	Backward Walking Slow: [-0.3, 0, 0, 0, 0, 0]; Forward Walking Slow: [0.3, 0, 0, 0, 0, 0]; Sidestep Left Slow: [0, 0.3, 0, 0, 0, 0]; Sidestep Right Slow: [0., 0.3, 0, 0, 0, 0]; Spin Clockwise Slow: [0, 0, 0, 0, 0, -0.8]; Spin Counterclockwise Slow: [0., 0, 0, 0, 0, 0.8]	1LVT+0.5AVT-1BH-1.5FC+1FAT- 2LVP-0.2BOP-0.01AR-0.01AS- 0.05AVP-0.0000025JA-0.00002JP- 0.000001JPD	No	$h_{target} = 0.25$ $p_{f,z,j}^{des} = 0.26$

Tab. S4. Definition of robot parameters and domain randomization.

Parameter (Dimension)	Unit	Randomization/Noise Range	Operator
Projected Gravity (3)	-	[-0.05, 0.05]	additive
Joint Position (12)	rad	[-0.03, 0.03]	additive
Joint Velocity (12)	rad/s	[-1.5, 1.5]	additive
Base Angular Velocity (3)	rad/s	[-0.3, 0.3]	additive
Base x-y Linear Velocity (2)	m/s	[-0.1, 0.1]	additive
Base Mass (1)	kg	[-1, 1]	additive
Kp Factor (12)	%	[0.9, 1.1]	scaling
Kd Factor (12)	%	[0.9, 1.1]	scaling

Tab. S5. Hyperparameters of PPO algorithm.

Hyperparameter	Value
Actor hidden size	[512, 256, 128]
Critic hidden size	[512, 256, 128]
CEN encoder hidden size	[128, 64]
CEN decoder hidden size	[64, 128]
CEN hidden state dim	16

AMP discriminator hidden size	[1024, 512]
Learning rate	Adaptive
Optimizer	Adam
Value loss clipping	True
Learning epochs per iteration	5
Minibatch size	6144
Discount factor	0.99
GAE factor	0.95
Maximum gradient norm	1

Tab. S6. Hyperparameters of the RSG inference and composition.

Hyperparameter	Value
High match threshold α_{high}	0.9
Low match threshold α_{low}	0.7
Mean function m_0	0
Parameters of the kernel function σ_f, l	2, 1
Measurement noise standard deviation σ_{noise}	10^{-4}

Algorithm S1. RSG inference and composition.

<p>Initialization: Given environment and task query q_{env}, q_{task}; The constructed RSG Ω; Matching threshold with skills existing in SG $\alpha_{high}, \alpha_{low}$; The score function $\mathbb{S}(\bullet)$.</p> <ol style="list-style-type: none"> 1. Calculate match $s = \mathbb{S}(q_{env}, q_{task})$. 2. Return matched skills $[A_0, \dots, A_N] = \Omega(s)$. 3. If $s \geq \alpha_{high}$: Reuse the best matching skills A_0. 4. Elif $s \leq \alpha_{low}$: The skills $[A_0, \dots, A_N]$ are used as the initial value, which is further fine-tuned by the RL algorithm. 5. Else: Initialize BO weight $w_0 = s, b = 0$. Update BO weight by maximize the new accumulated reward.
--

REFERENCES

1. Rudin, N., Hoeller, D., Reist, P., & Hutter, M. (2022, January). Learning to walk in minutes using massively parallel deep reinforcement learning. In Conference on Robot Learning (pp. 91-100). PMLR.
2. Made Aswin Nahendra, I., Yu, B., & Myung, H. (2023). DreamWaQ: Learning Robust Quadrupedal Locomotion with Implicit Terrain Imagination via Deep Reinforcement Learning.

- nforcement Learning. arXiv e-prints, arXiv-2301. Margolis, G. B., & Agrawal, P. (2023, March).
3. Walk these ways: Tuning robot control for generalization with multiplicity of behavior. In Conference on Robot Learning (pp. 22-31). PMLR.